2013

EXPERIMENTAL COMPARISON STUDY OF THE RESPONSE OF POLYCARBONATE AND LAMINATED GLASS BLAST RESISTANT GLAZING SYSTEMS TO BLAST LOADING

Joshua Calnan
University of Kentucky, josh.calnan@gmail.com

STUDENT AGREEMENT:

I represent that my thesis or dissertation and abstract are my original work. Proper attribution has been given to all outside sources. I understand that I am solely responsible for obtaining any needed copyright permissions. I have obtained and attached hereto needed written permission statements(s) from the owner(s) of each third-party copyrighted matter to be included in my work, allowing electronic distribution (if such use is not permitted by the fair use doctrine).

I hereby grant to The University of Kentucky and its agents the non-exclusive license to archive and make accessible my work in whole or in part in all forms of media, now or hereafter known. I agree that the document mentioned above may be made available immediately for worldwide access unless a preapproved embargo applies.

I retain all other ownership rights to the copyright of my work. I also retain the right to use in future works (such as articles or books) all or part of my work. I understand that I am free to register the copyright to my work.

REVIEW, APPROVAL AND ACCEPTANCE

The document mentioned above has been reviewed and accepted by the student's advisor, on behalf of the advisory committee, and by the Director of Graduate Studies (DGS), on behalf of the program; we verify that this is the final, approved version of the student's dissertation including all changes required by the advisory committee. The undersigned agree to abide by the statements above.

Joshua Calnan, Student

Dr. Braden T. Lusk, Major Professor

Dr. Thomas Novak, Director of Graduate Studies

EXPERIMENTAL COMPARISON STUDY OF THE RESPONSE OF POLYCARBONATE AND LAMINATED GLASS BLAST RESISTANT GLAZING SYSTEMS TO BLAST LOADING

THESIS

A thesis submitted in partial fulfillment of the requirements for the degree of Master of Science in Mining Engineering in the College of Engineering at the University of Kentucky

By

Joshua Thomas Calnan

Lexington, Kentucky

Director: Dr. Braden T. Lusk, Associate Professor of Mining Engineering

Lexington, Kentucky

2013

ABSTRACT OF THESIS

EXPERIMENTAL COMPARISON STUDY OF THE RESPONSE OF POLYCARBONATE AND LAMINATED GLASS BLAST RESISTANT GLAZING SYSTEMS TO BLAST LOADING

Abstract

This thesis recounts the experimental study of the dynamic response of polycarbonate blast resistant glazing systems to explosive loading through the use of triaxial load cells, pressure sensors, and a laser displacement gauge. This instrumentation captured the response of the glazing systems to blast loading over three phases of testing. The first phase of testing characterizes the load distribution around the perimeter and the second phase examines the repeatability of the results. The final phase of testing pushes the samples to failure. The results are then compared to HazL, a commonly used blast resistant glazing system analysis software tool. The experimental data is also compared to data available characterizing the response of laminated glass.

KEYWORDS: Polycarbonate, Laminated Glass, Blast Loading, Blast Resistant Glazing System, Dynamic Response

Joshua Thomas Calnan

4/18/2013

EXPERIMENTAL COMPARISON STUDY OF THE RESPONSE OF POLYCARBONATE AND LAMINATED GLASS BLAST RESISTANT GLAZING SYSTEMS TO BLAST LOADING

By

Joshua Thomas Calnan

Dr. Braden T. Lusk
Director of Thesis

Dr. Thomas Novak
Director of Graduate Studies

4/18/2013

DEDICATION

I dedicate this thesis to the men, women, children, and emergency personnel, who lost their lives in the Alfred P. Murrah Federal Building bombing on April 19, 1995 and in the terrorist attacks of September 11, 2001. I also dedicate this thesis to the men and women who serve to protect this nation from all threats, foreign and domestic. My hope is that the information presented in this thesis may one day be used to help prevent the future loss of life.

Finally, I would like to dedicate this thesis to my family. Without their help and support none of this would be possible.

ACKNOWLEGMENTS

The following thesis benefited from help of many people. First, I would like to thank my Thesis Chair, Dr. Braden Lusk, for his guidance and support throughout the completion of this thesis. I would also like to thank Dr. Kyle Perry, Joshua Hoffman, Rex Meyr, and the rest of the University of Kentucky Explosives Research Team for the assistance they provided me throughout the thesis process. I would also like to thank Dr. L. Sebastian Bryson for being part of my Thesis Committee. Each individual provided insights that guided me to improving the finished product.

In addition to the technical assistance given to me by those above, I received equally important support and encouragement from my family and friends. My fiancée, Courtney, provided encouragement throughout the process. Without her support (and patience) this would not have been possible. My parents, Tom and Cori, instilled in me the desire to continue my education and have supported me from the beginning.

TABLE OF CONTENTS

LIST OF TABLES

LIST OF FIGURES

Chapter One: Introduction

In the years following the World Trade Center Bombing in 1993, the Alfred P. Murrah Federal Building bombing in Oklahoma City in 1995, and the terrorist attacks on September 11, 2001, protection from human made threats has been a growing concern throughout the nation and the world. At the forefront of these concerns is protection from large blast events. Within the United States, numerous blast events occur every year. However, most are small, involving less than 10 pounds of high explosive. When large blasts do occur, there is usually significant structural damage, personal injury and death.

During the Oklahoma City bombing, 200 people outside the Alfred P. Murrah building were directly injured by flying or falling glass. This accounts for 39% of the total 508 injured (Norville, 2006). The use of properly design blast resistant glazing systems (BRGS) in high risk targets and surrounding structures can significantly reduce the severity and number of injuries should a blast event occur in the future.

1.1 Thesis Problem Statement

Static design methods and computer modeling techniques tend to be overly conservative in predicting the design strength of glazing systems. While this may be beneficial in ensuring that the glazing system will withstand a given blast loading, it may present challenges in adequately determining the load transferred to surrounding structural supports. Current structural design methodology uses a load path approach, with the required strength of a given element being calculated based on the loads transmitted to it by connecting

elements. If the transmitted loads are underestimated, it may be possible to overload elements further down the load path. Such is the case with blast resistant glazing systems. If the glazing material does not yield as predicted, greater loading than anticipated will be transmitted to the framing material and connecting structural elements, which if not of adequate strength, could fail resulting in severe structural damage.

The purpose of this thesis is to investigate the reaction forces transmitted by a blast resistant glazing system (BRGS) to the surrounding support members when subjected to blast loading. Three phases of testing were conducted on two different polycarbonate samples with thicknesses of one quarter (1/4) inch and one half (1/2) inch. The reaction force and deflection data collected from these polycarbonate samples were compared to each other as well as compared to data collected from a similar study conducted by W. C. Wedding on laminated glass load transfer (Wedding, 2010).

The first phase of testing characterized the reaction forces around the perimeter of the BRGS. Triaxial load cells were placed at the corners and midpoints of all four edges of a rectangular window to determine the magnitude of the reaction forces and also distribution of the forces. These results were compared to the distribution results gathered from the laminated glass study.

The second phase of testing determined the repeatability of the measurements. Consistent results were obtained with little variation in reaction forces. Using this information along with the information gathered in the first

phase of testing, it may be possible to characterize the load transfer of the future BRGS with a fewer number of tests.

The final phase of testing took the samples to failure. This phase measured the peak reaction forces transmitted to the support members prior to failure of the BRGS. This information was also compared to laminated glass.

The objective of this thesis was to record and analyze the reaction forces and deflection of a polycarbonate blast resistant glazing system subjected to blast loading. This information was then used to determine the peak loading and characterize the load transfer. These results were then compared to similar tests characterizing the load transfer of a laminated glass blast resistant glazing system.

Chapter Two: Background Information

2.1 The Nature of Blast Loading

An explosion is defined as a large-scale, rapid and sudden release of energy (Ngo et al., 2007). Explosions may be categorized as either physical, nuclear, or chemical explosions. Physically explosions are typically associated with the catastrophic failure of a containment vessel, whether it be a ruptured compressed gas cylinder or an erupting volcano. Nuclear explosions are caused by the redistribution of the protons and neutrons within atomic nuclei. This formation of different nuclei results in a large release of energy. The detonation of high explosives can be categorized as a chemical explosion which is the result of rapid oxidation of carbon and hydrogen atoms (Ngo et al., 2007).

Detonation of high explosives generates hot gases under high pressure. As these hot gases expand rapidly, forcing air out of the occupied space, a shock wave forms in front of this expanding volume. The overpressure, or increase in pressure above ambient pressure, associated with a blast event is the result of this shock wave. Shortly after the shock wave passes, a partial vacuum is created, sucking air back towards the blast source. This is referred to as the negative phase (Ngo et al., 2007). The negative phase is often ignored but can prove to be just as dangerous as the positive phase as damaged and broken windows can be sucked out their openings, injuring individuals outside of a structure.

Figure 2.1 shows a typical blast pressure profile, known as a Friedlander Curve. Prior to the time of arrival, t_A, the ambient air pressure can be expressed

as $P_{o.}$ At the time of arrival, the pressure suddenly increases to a peak overpressure value, P_{so}. The pressure then decays back to the ambient pressure. This duration is the positive phase duration, expressed using the term t_d. The pressure continues to decrease below the ambient air pressure until it reaches the peak negative pressure, P_{so}^-. The pressure eventually returns back to ambient pressure. This is expressed as t_d^-, or the negative phase duration. The negative phase is generally longer than the positive phase but of a much lower intensity. Impulse of a blast wave is equivalent to the sum of the area under the pressure curve, otherwise known as integration of the pressure versus time curve. (Ngo et al., 2007).

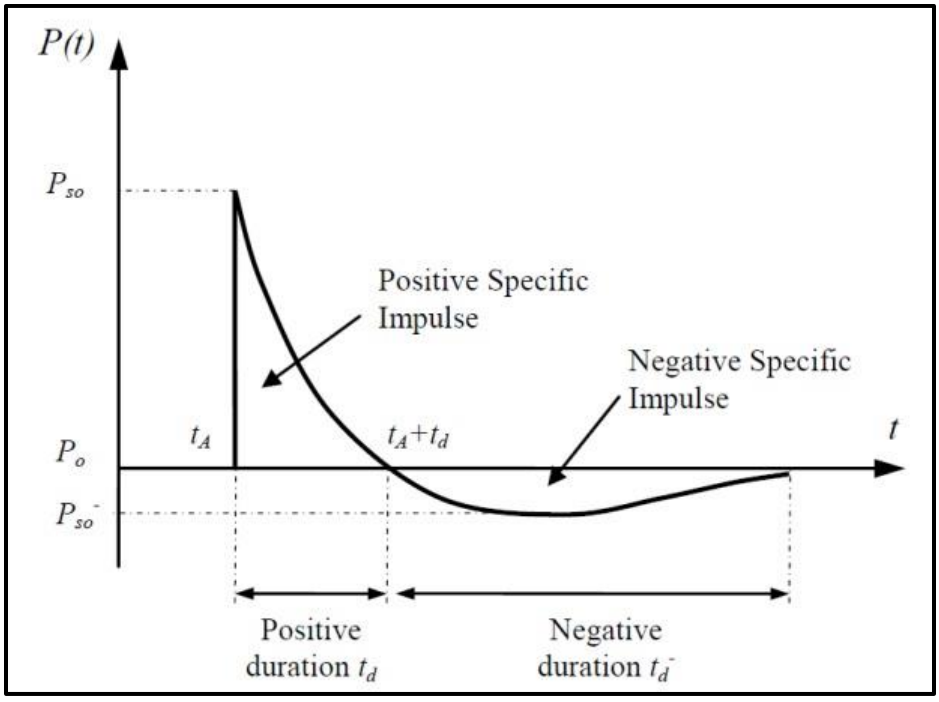

Figure 2.1: Blast wave Pressure - Time history (Ngo et al., 2007)

Standoff distance and charge size are major factors in determining the pressure and impulse exerted on a structure by a blast event. As standoff distance increases, so too does the duration of the positive phase, although at a lower intensity. Pressure and impulse will also be influenced by objects and structures as the blast wave is reflected and the peak overpressure is amplified (Ngo et al., 2007). Reflection sources can include the ground or any structure with sufficient mass so that it does not experience significant movement during the duration of the impulse loading (Dusenberry, 2010). The blast waves caused by an explosion at or near ground level are regarded as an expanding hemisphere with the greatest and most concentrated pressures and impulses occurring when the hemisphere is still of a small radius. As the radius of the hemisphere expands, it becomes increasingly planar, imparting lower pressures and impulses over a wider area.

2.2 Blast Resistant Glazing System Components

Blast resistant glazing systems serve a number of purposes. In the majority of cases, blast resistant glazing systems will never experience a blast loading. Therefore, one of its primary purposes must be to act as standard glazing, remaining aesthetically pleasing, allowing occupants of building views of the outside, and also meeting thermal, sound, and energy requirements. However, blast resistant glazing must minimize laceration hazards associated with flying and falling glass shards and maintain closure of the glazed opening.

Annealed float glass is the most commonly used glass in windows but is brittle and provides little resistance to blast loading. When annealed glass

breaks it forms many large, jagged, sharp fragments that can travel at high velocity. After breakage, the window is unstable with no remaining structural integrity (Stiles, 2010). Figure 2.2 illustrates the breakage pattern associated with annealed glass.

Figure 2.2: Annealed glass breakage pattern (Stiles, 2010)

Tempered glass is approximately four times stronger than annealed glass and is much more impact resistant. When broken, tempered glass shatters into many small rounded pieces that are less likely to cause harm. These small pieces are a result of the surface tension caused by the tempering process. Tempered glass is commonly used in applications because of its increased safety rather than its increased strength. Like annealed glass, once tempered glass is broken, it has no remaining structural integrity (Stiles, 2010). Figure 2.3 shows the breakage pattern common with tempered glass.

Figure 2.3: Tempered glass breakage pattern (Stiles, 2010)

Wire glass is commonly used in fire rated doors but provides little blast protection. In fact, once broken, the exposed wire within the glass can pose as much of a risk as the annealed glass itself. As illustrated in Figure 2.4, wire glass breaks into large sharp fragments like traditional annealed glass, but the wire may hold some pieces within the frame (Stiles, 2010).

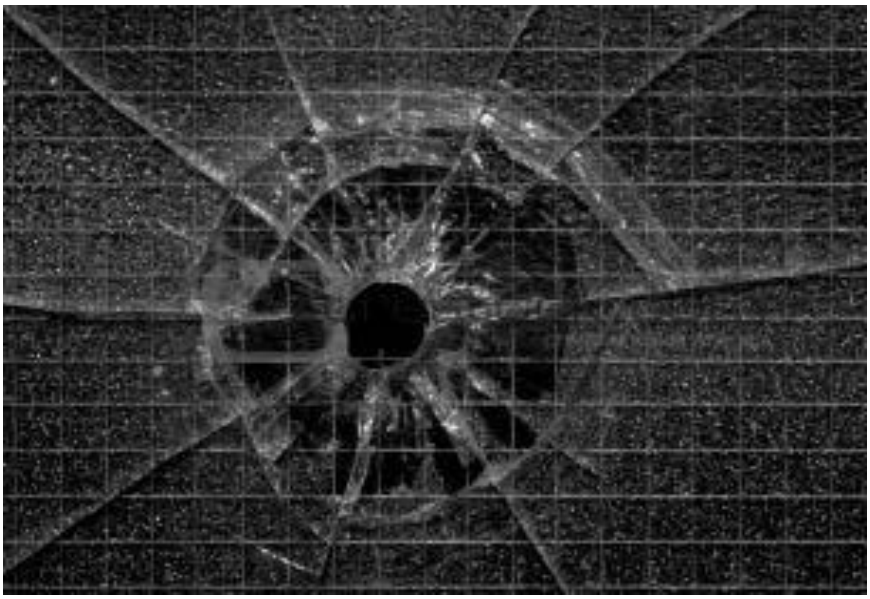

Figure 2.4: Wired glass breakage pattern (Stiles, 2010)

The most common glazing material for blast protection is laminated glass. Laminated glass is constructed of a polymer layer, usually polyvinyl butyral (PVB), bonded between layers of glass. PVB interlayer thickness can range from 0.015 inches to 0.10 inches depending on the application (Stiles, 2010). Annealed glass is typically used although tempered glass can be used when increased initial strength is required. The PVB layer is effective at retaining the glass fragments and the laminated glass continues to exhibit significant resistance to blast loading even after the window has shattered. When impact and ballistic strength is also of a concern, polycarbonate can be used in the laminate (Hooper, 2011).

When subjected to blast loading, laminated glass initially responds as an elastic plate, much like a monolithic pane. This is called the precrack phase. Following the precrack phase, the tensile stress becomes strong enough that cracks begin to occur and propagate from flaws in the glass layer. Once the

glass has fractured, it enters the postcrack phase. During this time the deflected shape of the window shows a flat central region with curved regions concentrated at the edges. As the window continues to deflect, the flat region becomes smaller until eventually the entire profile is curved. In this phase the glass fragments remain bonded to the polymer interlayer, continuing to provide resistance to the blast loading. At this point the laminate behaves as a membrane and is able to withstand large deformations. Complete failure of the laminate occurs when the polymer interlayer tears (Hooper, 2011). An image of a broken laminated glass panel can be found in Figure 2.5.

Figure 2.5: Laminated glass breakage pattern (Stiles, 2010)

While the majority of the glass remains intact with laminated glass, spalling of smaller fragments may still be of concern. Anti-spalling requirements are separated into two levels; low spalling which allows for a limited amount of glazing loss, and non-spalling which allows for no glazing loss. When non-

spalling glass is required, anti-spalling film can be added to the back of laminated glass to prevent any glazing loss (Stiles, 2010).

Polycarbonate is a lightweight synthetic material. It is becoming more common in blast resistant glazing systems because it offers 250 times the breakage resistance of equal thickness annealed glass. Polycarbonate is susceptible to scratching and gouging and may exhibit slight yellowing if not UV treated (Stiles, 2010). Delamination and deformation may be visible once subjected to blast loading, but generally polycarbonate shows no signs of breakage.

Glass clad polycarbonate are comprised of glass, PVB, and polycarbonate. The polycarbonate may be sandwiched between the glass layers for scratch resistance or it may be laminated to the backside of the glass for spalling protection. Glass clad polycarbonate behaves much like traditional laminated glass with the glass layers cracking but the window retaining structural integrity (Stiles, 2010).

Regardless of the glazing material, the attachment points and supporting structure must be of ample strength to prevent the pane from detaching and entering the building at a high velocity. Structural silicone sealant is most commonly used for bonding the glazing material to the framing structure but structural tape may be used as well. Glazing blocks also serve to keep glazing in place in some cases. Through bolting is generally discouraged as stresses to concentrate around the holes. In commercial buildings, extruded aluminum alloy is commonly used as the framing material with the glazing material restrained at

two or four of its edges. Steel may also be used if loads dictate or if long clear spans are required. It is recommended to secure the glazing material on both sides with structural silicone at all four edges (Hooper, 2011). Frame bite, the distance the glazing material overlaps the framing material, is also a concern and is dependent on the type of glazing material used and the anticipated blast loading.

2.3 Blast Design

The first step in designing any blast resistant structure is determining the threat. For explosives manufacturing and storage facilities, this is a relatively straightforward process as the amount and type of explosives present, along with standoff distances are known. This is also true for military installations and embassies, where the type of possible threat is usually known. Risk and threat assessments for commercial and private buildings pose a more significant challenge. There are a number of uncertainties when predicting a terrorist threat, such as type of explosive used, charge size, and standoff distance. All of which are critical to properly characterizing a blast loading (Stewart, 2007).

It is not economically feasible to protect a structure from all possible threats. A probabilistic risk assessment should be conducted to predict the risks associated with a blast event. These risks must then be quantified and compared in a consistent and rational manner. It is then possible to determine which threats are most significant and can be economically mitigated (Stewart, 2007). Once the threats have been identified, the required blast mitigation techniques may be specified.

For external explosion threats, the building facade, including the glazing system, is the first line of defense for protecting the building as a whole. Not only does the facade protect the occupants of a building, it also protects the building by preventing blast waves from entering the structure. Blast waves that enter the structure can threaten interior floors, walls, and columns and pose a significant risk to elements such as floor systems that are designed only to support downward gravity loads. By designing a facade and glazing system that prevents the blast wave from entering the building, the engineer must in turn provide ample strength to the structure in order to support the blast loading while keeping levels of damage at acceptable levels (Dusenberry, 2010).

Blast loading differs significantly from loadings generally analyzed by structural engineers and architects. The pressures associated with these loadings are orders of magnitude greater than those commonly designed for and also have much shorter durations, usually in the millisecond range. Many times engineers believe that they can apply standard design methods used in non-blast loading scenarios. In traditional static design scenarios, the stress level of a component is limited so that it remains within its elastic limits. In blast design this is not the case. Instead, limits are placed on the maximum allowable dynamic deflection, resulting in controlled, ductile yielding. The amount of allowable deflection is based on whether repairable or unrepairable damage is acceptable. Complete failure of the component is generally not an option (Dusenberry, 2010).

The risk of an explosion at any single structure is often very low and the costs to achieve an elastic response are very high. Therefore, design of these

structures generally relies on the energy-dissipating capabilities of the structural elements with deformations well into the inelastic range of the element. As a blast wave strikes the building facade it is instantaneously reflected, imparting kinetic energy to the components. This energy must either be absorbed or dissipated to prevent failure of the associated components. This is done by converting the kinetic energy within the component to strain energy in the restraining elements (Dusenberry, 2010).

The primary challenge faced by engineers is determining the response of windows to blast loading. Currently, this is calculated using government-sponsored software that is not generally available to the public. These programs, including HazL (Window Fragment Hazard Level Analysis) and Wingard (Window Glazing Analysis Response and Design), model the window response using an equivalent single degree of freedom (SDOF) system for a number of common window configurations. Static design equivalents such as ASTM F2248 (ASTM, 2012b) and E1300 (ASTM, 2012a) may also be used. (Dusenberry, 2010).

Analyzing the dynamic response of a blast-loaded structure is a complex task that involves the effect of high strain rates, non-linear inelastic material behavior, uncertainties of load calculations, and time-dependent deformations. A number of assumptions can be made to simplify the analysis process including idealizing the glazing system as a single degree of freedom (SDOF) system. The BRGS is replaced by an equivalent system of a concentrated mass and a spring which represents the resistance of the BRGS against deformation. The mass is represented by M which is being acted on by an external force over a period of

time, F(t). The resistance is represented by R and expressed in terms of vertical displacement as represented by y, and the spring constant, K. Figure 2.6 provides an illustration of this simplified system. The blast load is idealized as a triangular pulse with a peak force of F_m and a positive duration of t_d. This simplified blast load is shown in Figure 2.7. The external force is calculated using the following equation:

$$F(t) = F_m\left(1 - \frac{t}{t_d}\right) \quad 2.1$$

The impulse is approximated as the area under the force-time curve and can be calculated using the following equation:

$$I = \frac{1}{2}F_m t_d \quad 2.2$$

The equation of motion for an un-damped elastic SDOF system is expressed as:

$$M\ddot{y} + Ky = F_m\left(1 - \frac{t}{t_d}\right) \quad 2.3$$

The displacement and velocity of the glazing system can be expressed as shown in Equations 2.4 and 2.5 where velocity is simply the derivative of displacement:

Displacement

$$y(t) = \frac{F_m}{K}(1 - cos\omega t) + \frac{F_m}{Kt_d}\left(\frac{sin\omega t}{\omega} - t\right) \quad 2.4$$

Velocity

$$\dot{y}(t) = \frac{dy}{dt} = \frac{F_m}{K}\left[\omega sin\omega t + \frac{1}{t_d}(cos\omega t - 1)\right] \quad 2.5$$

The natural frequency of the structure is defined as ω and T is the natural period of vibration for the structure. The natural frequency of the structural can be calculated using the equation:

$$\omega = \frac{2\pi}{T} = \sqrt{\frac{K}{M}} \qquad 2.6$$

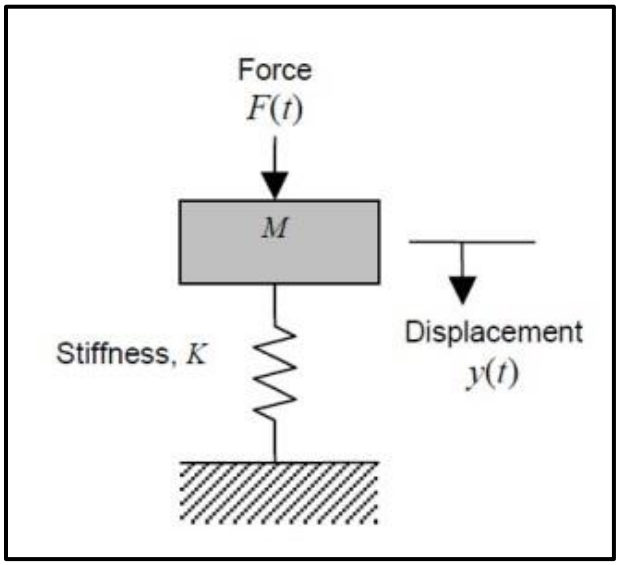

Figure 2.6: Representation of a Single Degree of Freedom (SDOF) system (Ngo et al., 2007)

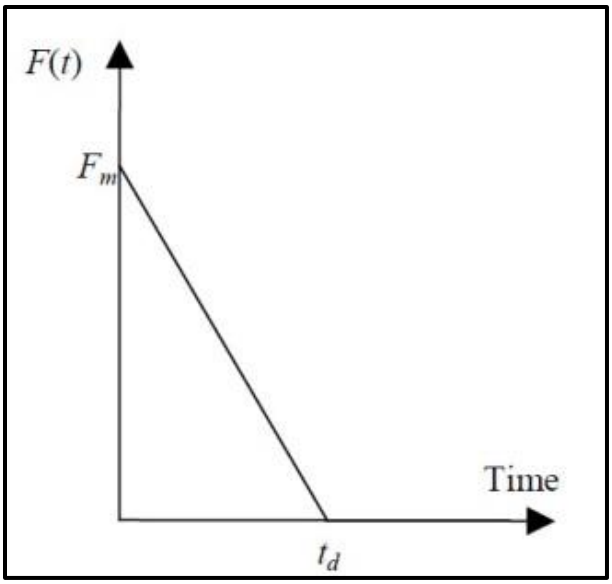

Figure 2.7: Simplified blast loading used for SDOF analysis (Ngo, et al., 2007)

The maximum response of the structure is equal to the maximum deflection of the structure, $y_{m,}$ which occurs at time t_m. If the velocity of the system is set to zero, then it is possible to determine a value for t_m. It then becomes possible to obtain the displacement of the structure by substituting t_m into Equation 2.4 (Ngo et al.,2007). Dampening has little effect on the displacement of the structure and it generally ignored for these calculations (Stewart, 2007).

2.4 Design Guidelines and Standards

There are currently two standards used to aid in blast-resistant glazing design. They are Standard 10 of UFC 4-010-01 (DoD, 2012) and ASTM F 2248-12 (ASTM, 2012b). Prior to 2012, the UFC provided design guidelines assuming certain standoff distance requirements were met and the structure was at a secure facility. In the most current revision, UFC 4-010-01 9 February 2012, set

standoff distances are not specified. This change requires the engineer to analyze each glazing system on a case by case basis, rather than designing a glazing system to a set standard. ASTM F 2248-12 uses a 3-second equivalent design load to size the glass and determine the loading that must be supported by the framing and its connections.

Prior to 2012, the UFC standard applied to two charge weights and associated minimum standoffs with Explosive Weight I having a pressure and impulse of 4.8 psi and 41.1 psi-ms and Explosive Weight II having a pressure of 5.8 psi and impulse of 29.7 psi-ms. The exact charge weights and standoff distances cannot be published. For charges of greater weight and lesser standoff distances a detailed analysis or blast testing was required. Using the current UFC standard essentially removes these blast loading scenarios, allowing more flexibility in the layout of the building, but increases the challenges faced by the glazing system designer.

Regardless of the blast loading scenario, the UFC recommends a minimum nominal thickness of 1/4 inch laminated glass composed of two 1/8 inch glass plies bonded with a 0.030 in PVB interlayer. If insulated glass is used, the inner lite should be composed of 1/4 inch laminated glass. A minimum frame bite of 3/8 inch is recommended for structural silicone glazing and 1 inch for dry glazed systems. For the design of framing members and their connections, the UFC specifies that they must be able to withstand 2 times the glazing capacity specified per ASTM F2248. Prior to 2012, the UFC based the design requirements on the blast loading, rather than the glazing capacity.

ASTM F 2248-12 uses a 3-second equivalent based on work presented by Norville and Conrath (Norville, 2001). This chart can be found in Figure 2.8. Originally, this work related charge size and standoff distance to a 60-second equivalent design loading for use with laminated glass. This was changed to a 3-second equivalent to remain consistent with ASTM E 1300 (ASTM, 2012a). When used with E 1300, ASTM F 2248 provides guidelines for designing blast-resistant glazing including sizing the glass, and determining the required framing and connections.

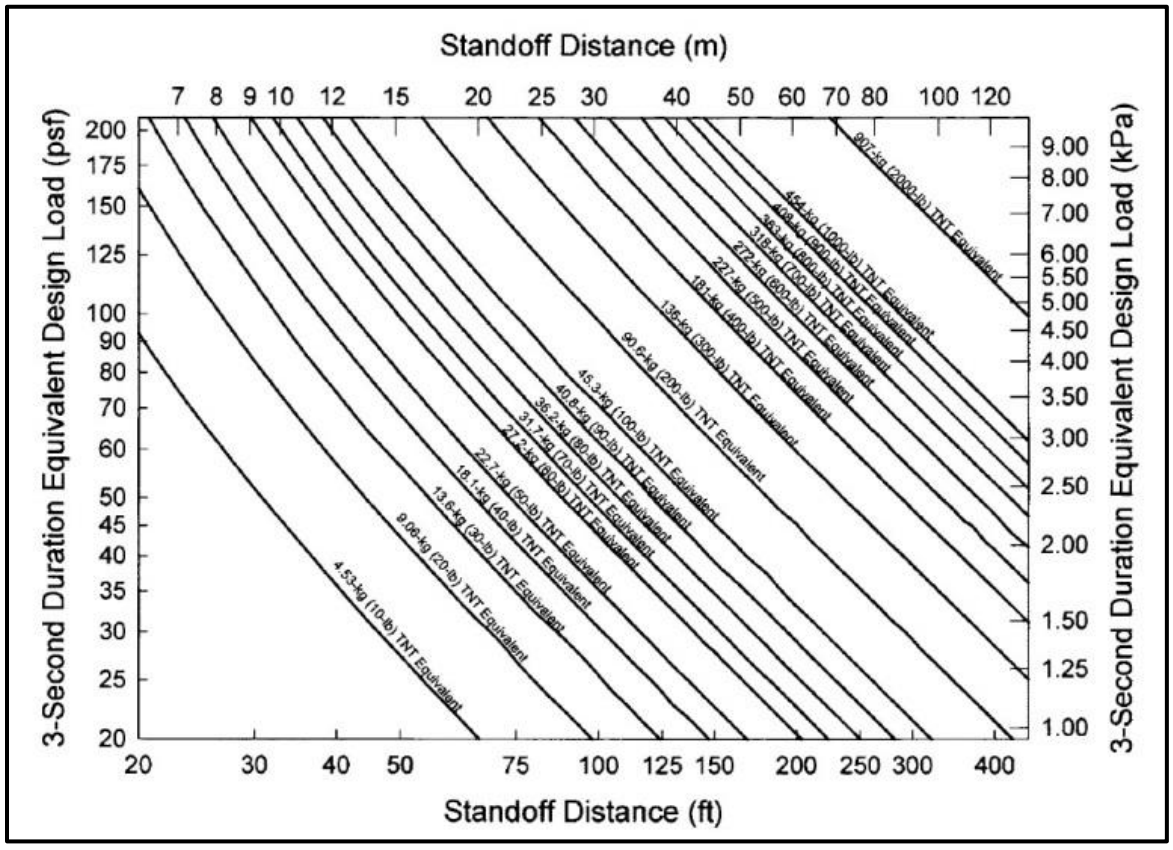

Figure 2.8: 3-Second equivalent design loading chart from ASTM F 2248-03 (ASTM, 2003)

In addition to the design guidelines provided in UFC 4-010-01 and ASTM F 2248, the federal government has specifications in place for categorizing the levels of safety provided by a BRGS during testing. The US General Services Administration (GSA) sets specifications for federally owned or leased buildings while the specifications for Department of Defense facilities are contained in UFC 4-010-01. Figure 2.9 shows an illustration of the GSA/ISC performance conditions. Performance is based on which zone within the witness area fragments are found. Table 2.1 provides the performance condition and associated description of the glazing response. Figure 2.10 and Table 2.2 provide similar information for the UFC specification.

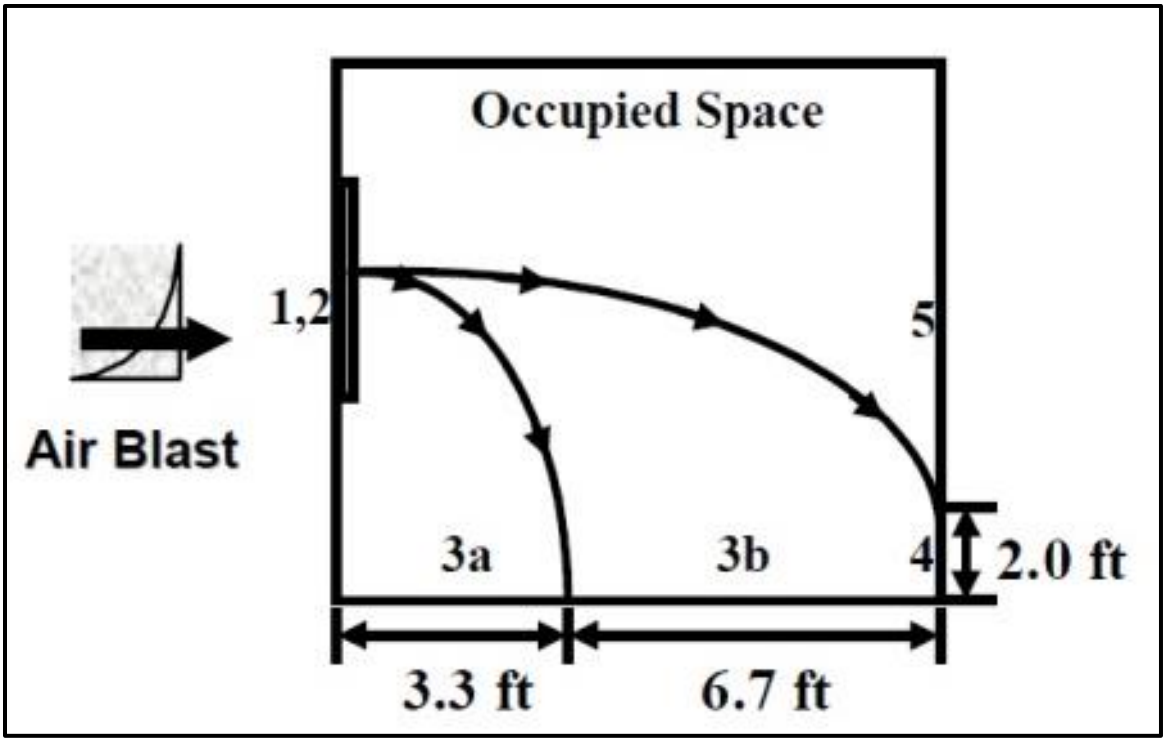

Figure 2.9: GSA/ISC performance conditions for window system (GSA, 2003)

Table 2.1: GSA/ISC performance conditions chart (AAMA, 2006)

Performance Condition	Protection Level	Hazard Level	Description of Window Glazing Response
1	Safe	None	Glazing does not break. No visible damage to glazing or frame.
2	Very High	None	Glazing cracks but is retained by the frame. Dusting or very small fragments near sill or on floor acceptable.
3a	High	Very Low	Glazing cracks. Fragments enter space and land on floor no further than 1 m (3.3 ft.) from the window.
3b	High	Low	Glazing cracks. Fragments enter space and land on floor no further than 3 m (10 ft.) from the window.
4	Medium	Medium	Glazing cracks. Fragments enter space and land on floor and impact a vertical witness panel at a distance of no more than 3 m (10 ft.) from the window at a height no greater than 0.6 m (2 ft.) above the floor.
5	Low	High	Glazing cracks and window system fails catastrophically. Fragments enter space impacting a vertical witness panel at a distance of no more than 3 m (10 ft.) from the window at a height greater than 0.6 m (2 ft.) above the floor.

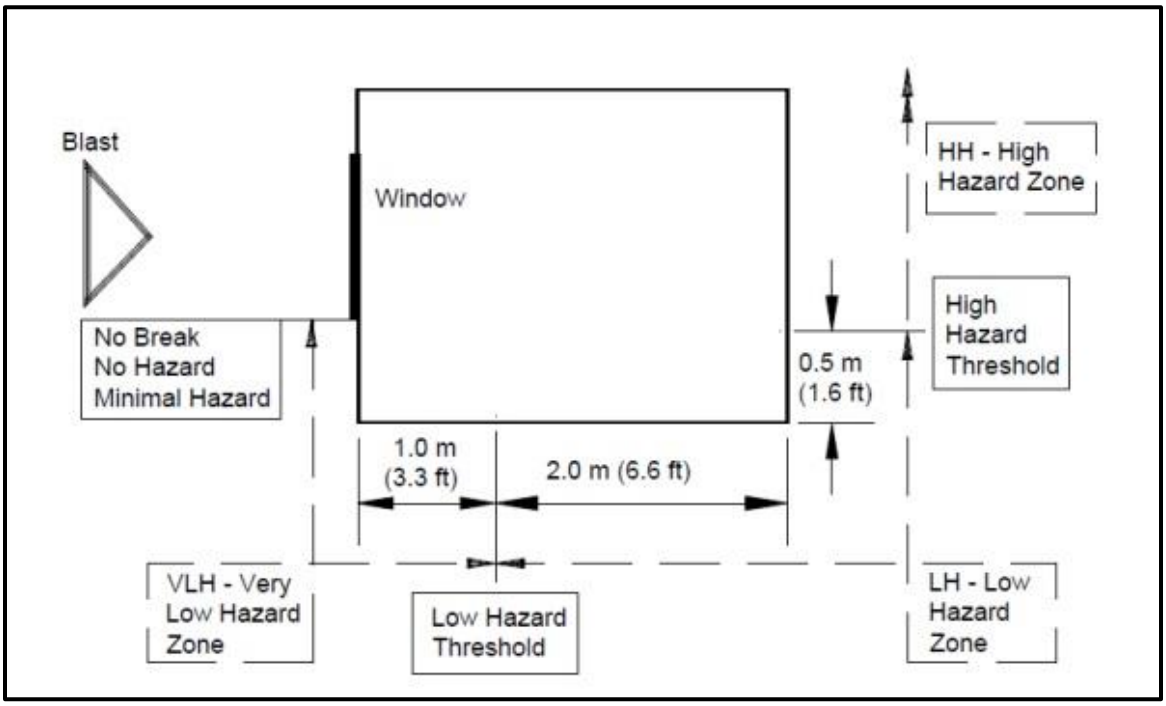

Figure 2.10: Illustration of DoD Window Hazard Levels for Blast Loaded Windows (ASTM, 2003)

Table 2.2: DoD Hazard Levels for Blast Load Windows (Adopted from ASTM 1642 by AAMA, 2006)

Hazard Level	Description of Fenestration Glazing Response
No Break	The glazing is observed not to fracture and there is no visible damage to the glazing system.
No Hazard	The glazing is observed to fracture but is fully retained in the facility test frame or glazing system frame and the rear surface (the side opposite the airblast loaded side of the specimen) is unbroken.
Minimal Hazard	The glazing is observed to fracture and the total length of tears in the glazing plus the total length of pullout from the edge of the frame is less than 20 % of the glazing sight perimeter. Also, there are three or less perforations caused by glazing slivers and no fragment indents anywhere in a vertical witness panel located 3 m (120 in.) from the interior face of the specimen and there are fragments with a sum total united dimension of 25 cm (10 in.) or less on the floor between 1 m (40 in.) and 3 m (120 in.) from the interior face of the specimen. Glazing dust and slivers are not accounted for in the rating. Fragments are defined as any particle with a united dimension of 2.5 cm (1 in.) or greater. The united dimension of a glass particle is determined by adding its width, length, and thickness. Glazing dust and slivers are all other smaller particles.
Very Low Hazard	The glazing is observed to fracture and is located within 1 m (40 in.) of the original location. Also, there are three or less perforations caused by glazing slivers and no fragment indents anywhere in a vertical witness panel located 3 m (120 in.) from the interior face of the specimen and there are fragments with a sum total united dimension of 25 cm (10 in.) or less on the floor between 1 m (40 in.) and 3 m (120 in.) from the interior face of the specimen. Glazing dust and slivers are not accounted for in the rating.
Low Hazard	The glazing is observed to fracture, but glazing fragments generally fall between 1 m (40 in.) of the interior face of the specimen and 50 cm (20 in.) or less above the floor of a vertical witness panel located 3 m (120 in.) from the interior face of the specimen. Also, there are ten or fewer perforations in the area of a vertical witness panel located 3 m (120 in.) from the interior face of the specimen and higher than 50 cm (20 in.) above the floor and none of the perforations penetrate through the full thickness of the foil backed insulation board layer of the witness panel as defined in ASTM F 1642 -04 Section 8.7.5.
High Hazard	Glazing is observed to fracture and there are more than ten perforations in the area of a vertical witness panel located 3 m (120 in.) from the interior face of the specimen and higher than 50 cm (20 in.) above the floor or there are one or more perforations in the same witness panel area with fragment penetration through the first layer and into the second layer of the witness panel.

2.5 Design Capacity vs. Actual Tested Capacity

It has been observed through many open air and shocktube tests, that the results provided using these methods are often overly conservative and the blast resistant glazing systems fail at loadings significantly higher than expected. A summary of 63 full-scale blast tests was compiled by Meyers et al. (Meyers, 1994). For these tests, a number of thermally tempered glass, laminated

tempered glass, and polycarbonate samples of various sizes were tested using open air and shocktube testing.

The first series of 36 tests took place during January 1986 at the Lovelace Shocktube (Meyers, 1986). During this test series 28 blast tests were conducted on 18 monolithic thermally tempered glass samples and eight blast tests were conducted on five laminated thermally tempered glass samples. In all, a total of eight different window types were tested. The samples were first tested at their designed blast load. Next at least one sample from each type was tested at a blast overpressure predicted to cause a 50 percent rate of failure. Finally, one sample from each type was tested at an overpressure predicted to cause a 99 percent rate of failure.

During testing, all of the monolithic tempered glass survived its design blast load and only one sample failed at the 50 percent rate of failure loading. All monolithic samples failed when tested at overpressures predicted to cause a 99 percent rate of failure. Testing of the laminated thermally tempered glass resulted in only one failure, even with blast overpressures predicted to cause a 99 percent rate of failure. It is believed that the one failure could be attributed to improper installation of the gasket used to retain the sample.

In 1987 and 1988, arena tests of five polycarbonate samples were conducted by the Army Corps of Engineers (DoS, 1987). Each pane, manufactured by a different manufacturer, was predicted to withstand a loading of 105 psi. At peak reflected pressures of between 96 to 100 psi all samples survived as anticipated.

The Department of State conducted additional arena tests on five polycarbonate samples in 1988 (DoS, 1989). The smallest samples, measuring 26 x 26 x 1.3 inches, had a maximum design capacity of 56.3 psi. Both samples survived a blast loading of 57.4 psi. Two 36 x 36 x 1.3 inch panels withstood a blast loading of 49.2 psi although they were only rated for 35.4 psi. Finally, a 40 x 40 x 1.3 inch panel was tested and survived a blast loading of 57.4 psi significantly higher than its design capacity of 31.5 psi.

Finally a series of tests were conducted in August 1991 at Ft. Polk, Louisiana (CoE, 1992). Three ¾ inch thick polycarbonate panels were subjected to a loading of 14.6 psi, at or above their predicted design capacity. All panels survived with center deflections less than predicted. Three laminated tempered glass panes were also tested. It is believed that the temperature of each pane was above 100° F. Therefore, Gerald Meyers and Donald Baldwin reduced the static design load by 75% to account for thermal effects, resulting in adjusted design loads of 10.5, 12.7, and 24.9 psi. All three samples survived a blast load of 13.5 psi (Meyers, 1994).

As these previous tests show, it is not uncommon for blast resistant glazing systems to withstand blast loadings significantly larger than their rated design capacity. For many of the systems tested, the samples were not taken to complete failure, leaving the question of what the ultimate glazing capacity may be.

Chapter Three: Instrumentation and Equipment Setup

Instrumenting a blast event can pose challenges as the events are highly dynamic and last only a few milliseconds. However, during this very short time frame, large amounts of energy are released and transferred. To characterize the response of blast resistant glazing systems to blast loading, these challenges must be overcome.

3.1 Pressure Time History Measurement

The pressure time history of each blast event is characterized using piezoelectric dynamic pressure sensors manufactured by PCB Piezotronics. Two model 102B18 flush mount sensors were used during testing. These sensors are capable of providing sampling rates up to 1 Mhz, with nearly non-resonant response at pressures up to 50 psi, making them ideally suited for this type of testing. To gain accurate pressure measurements, it is important to mount the pressure sensors as close as possible to the window being tested. Therefore it was decided to flush mount a sensor within the framing material on either side of the window samples. These sensors were placed at the midpoint of the vertical window span. Figure 3.1 shows the mounting location of the pressure sensors with respect to the sample being testing. The sensors were fitted with nylon nuts to prevent damage and then pressed into holes bored into the wood framing material. Once mounted, the sensors occupied the same plane as the polycarbonate surface. This is shown in Figure 3.2.

Figure 3.1: Mounting location of piezoelectric dynamic pressure

Figure 3.2: Detailed view of pressure sensor mounted in wood

3.2 Window Deflection Measurement

Window deflection measurements were obtained through the use of a laser distance gauge manufactured by Acuity Laser Measurement. This gauge has the ability to provide non-contact measurements of the window surface at sample rates up to 9.4 kHz. The gauge has two major elements, a visible laser transmitter and a CMOS sensor receiver. The gauge works by bouncing a visible laser beam off the window surface and then calculating the distance travelled based on the amount of time required for the laser beam to be detected by the CMOS sensor. Since the polycarbonate does not provide an ideal surface for the laser beam to reflect off of, white tape is placed at the midpoint of the window to act as a reflective surface.

The sensor is mounted on a tripod at a height equal to the midpoint of the window. To protect the sensor from damage caused by flying debris should the window fail, the sensor is placed to the side of test specimen. Sandbags were placed at the base of each leg to stabilize the tripod during testing. This can be seen in Figure 3.3. Trigonometric identities were used to adjust for the angular offset and accurately characterize the window's movement. During the failure testing phases, the laser gauge was not used as the risk of damage to the sensor was too great.

Figure 3.3: Laser distance gauge setup adjacent to the test sample

3.3 Window Reaction Force Measurement

The major focus of this thesis was to characterize the reaction forces around the perimeter of polycarbonate blast resistant glazing systems during blast loading. W.C. Wedding (Wedding, 2010) developed the methodology and much of the equipment required to tackle this undertaking. Prior to his work, the

research team had a great deal of experience with other measurement types, but none with reaction force measurements. As reaction force measurements were still relatively new to the research team, some uncertainties remained.

PCB Piezotronics manufactured the triaxial load cells selected for this test series. The model 261A03 load cells provide a calibrated reaction structure which eliminates the need to preload the sensors during installation. The X and Y axes provide shear measurements while the Z-axis measures tension, compression, and impact forces. The Z-axis is capable of measuring loads of ±10,000 lbf at a sampling rate of 10 kHz. The X and Y axes provide the same sampling rate but at a maximum of ±4,000 lbf. These capabilities are significantly higher than required by this test series.

In order to provide adequate support for the glazing system, attachment points were positioned at eight inch intervals around the perimeter of the window. Since it is not logistically possible due to the amount of cabling required or economically feasible to populate all 26 attachment points with a triaxial load cell, proxy load sensors were used to occupy attachment points where there was not a load cell present. These proxy sensors were designed and tested by W.C. Wedding (Wedding, 2010) to provide the same stiffness characteristics as the load cells which they were intended to imitate, minimizing the effect the proxy sensors would have on the overall readings. Each proxy sensor consists of a steel upper and lower half with an aluminum inner ring that provided the desired stiffness. The desired stiffness for the Z-axis is 40 lbf per µin and the 15 lbf per µin for the X and Y axes. The proxy sensors also have the same bolt pattern as

the triaxial load cells, allowing them to be easily moved around the perimeter of the test frame. Figure 3.4 shows a model of the proxy sensor created by W.C. Wedding.

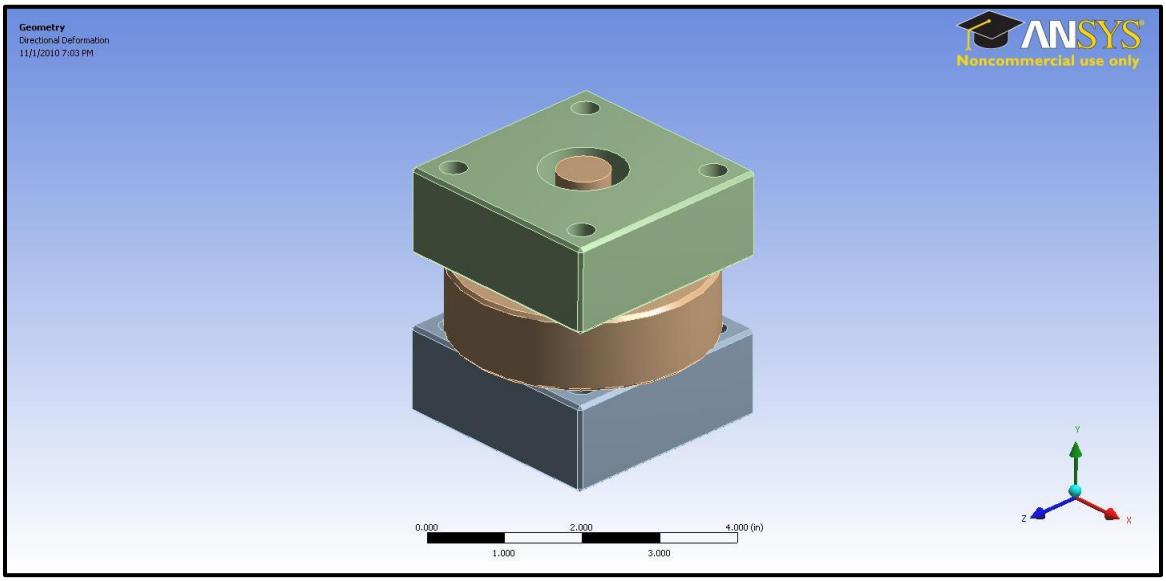

Figure 3.4: Ansys model used to illustrate the proxy sensors (Wedding, 2010)

The sensor brackets used to hold the triaxial load cells and proxy sensors in place around the perimeter of the window sample was also developed by W.C. Wedding. The brackets along the top and the bottom of the test fixture feature five attachment points with access holes for routing cables. The brackets for the sides of the test fixture are nearly identical in construction but feature eight attachment points. A model of the lower sensor bracket can be found in Figure 3.5.

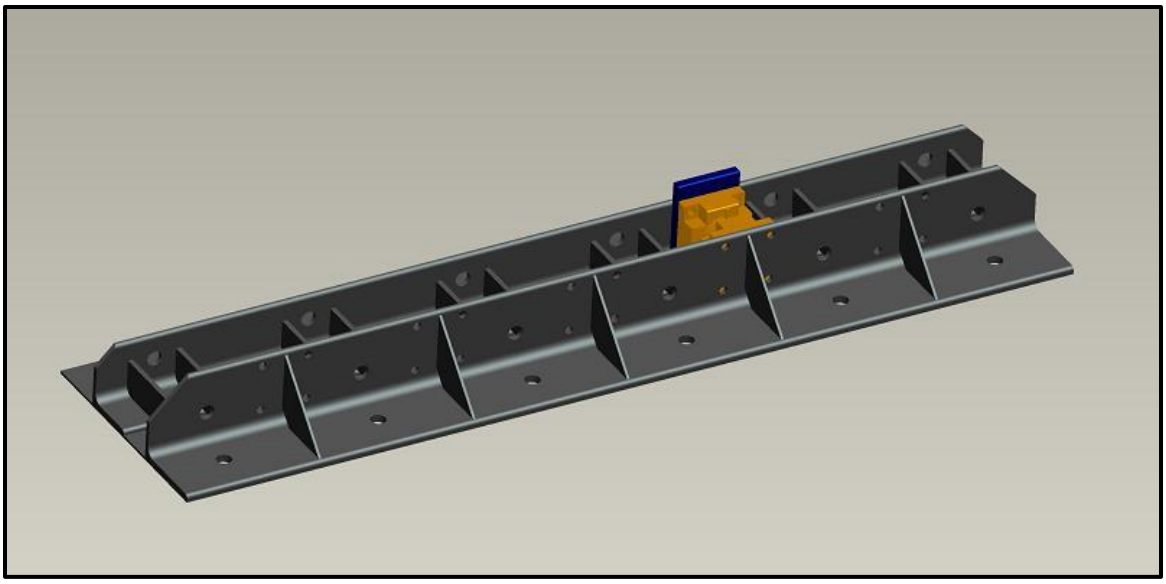

Figure 3.5: Model of upper and lower sensor bracket (Wedding, 2010)

3.4 Buck Design

A buck is an interchangeable end plate used on one end of the shock tube. The purpose of the buck is to allow the shock tube to be adapted to different test setups with relative ease. Each buck features four large diameter pins which seat into U-shaped saddles on the end of the shock tube. This allows the bucks to be lifted off and replaced with another. For this test series, a previously fabricated steel buck with a rectangular opening was utilized. The sensor brackets were bolted to the buck with wood shims used to adjust the opening to a final size of 47 ¾" wide x 66" tall. The wood shims also allowed the cabling for the pressure sensors to be passed through to the outside of the shock tube. The buck used for this test series is shown in Figure 3.6. In this image the buck is fully prepped for testing.

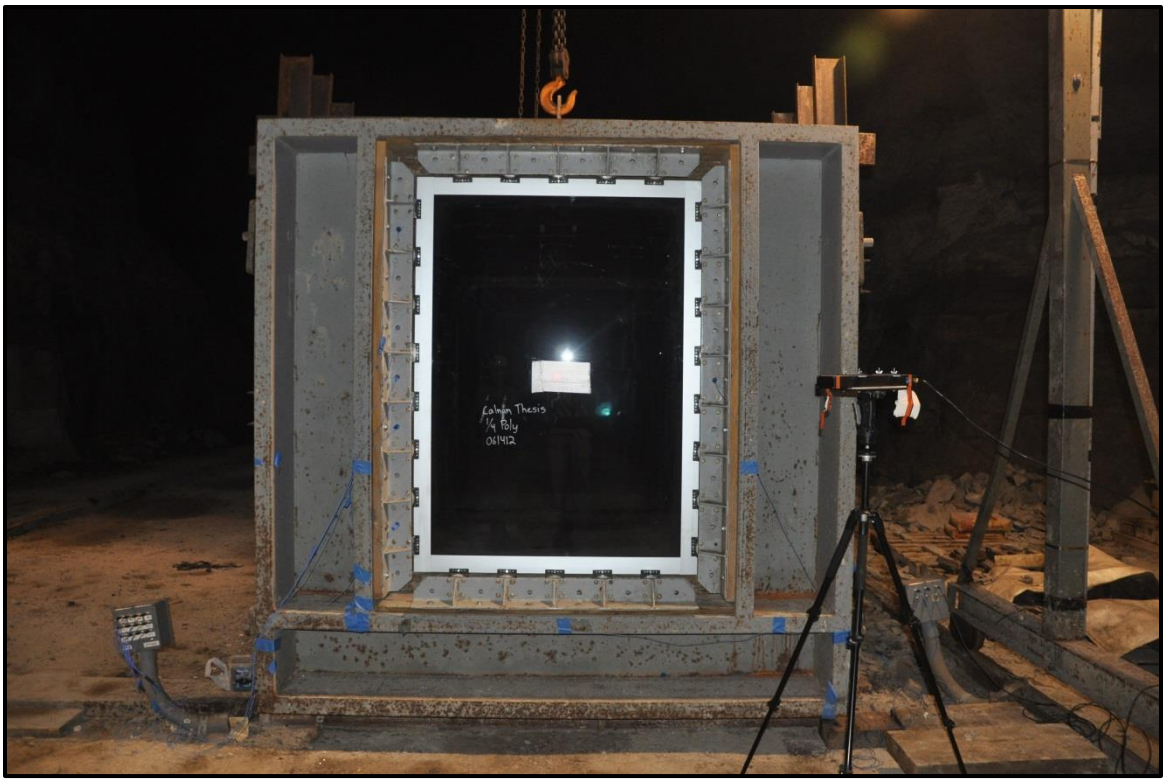

Figure 3.6: Buck fully prepared for testing

3.5 Data Acquisition Equipment

Data acquisition was a relatively straightforward process thanks to the use of a pair of Datatrap II acquisition devices manufactured by MREL. The Datatrap II is a ruggedized digital data recorder capable of capturing eight channels at rates up to 10 MHz. 15 data channels were required for this test series. Therefore, the pair of Datatraps were connected and synchronized in a master and slave configuration for simultaneous triggering and acquisition, allowing all 15 data channels to remain on the same time scale. The pressure sensor signals were routed to the master Datatrap and served as the trigger for the system.

A model 481A signal conditioner manufactured by PCB Piezotronics provided the necessary power regulation to the pressure sensors and triaxial load cells and served as the interface between these sensors and the Datatraps. The signal conditioner warns of any faults in the sensors and also protects against voltage and current overloads. The laser distance gauge provides its own power source and was connected directly to the Datatrap. After the data is retrieved from the Datatraps, it is copied into DPlot where calibration factors for each sensor are applied. This converts the data from voltages into pressure, deflection, or force. Figure 3.7 shows the suite of data acquisition devices used for testing including the signal conditioner, Datatraps, and laptop computer.

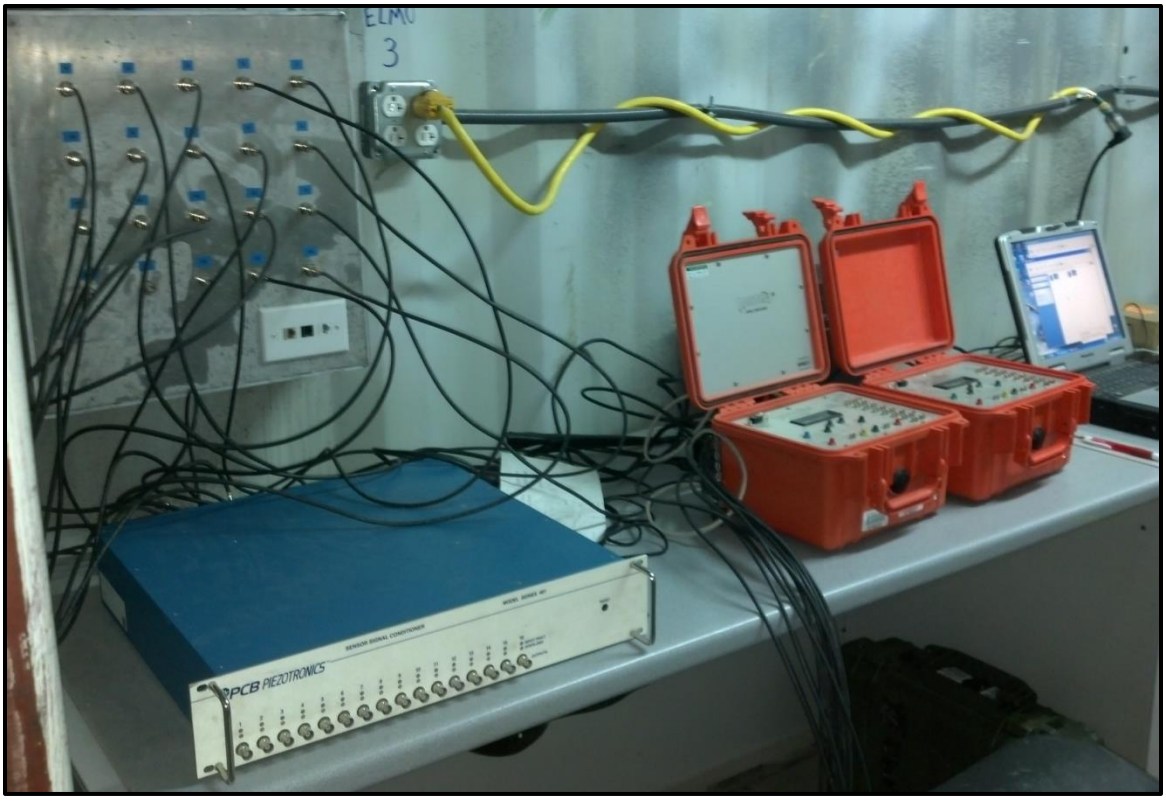

Figure 3.7: Data acquisition hardware

Chapter Four: Experimental Methodology

The experimental methodology used for this testing was largely based on the test methodology laid out by W.C. Wedding in his testing of laminated glass blast-resistant glazing systems (Wedding, 2010). The goal of this thesis was to determine the peak loading transferred to the support structure of a polycarbonate blast resistant glazing system as well as characterize the distribution of these loadings. The methodology utilized for this test series was a truncated version of that used by W.C. Wedding. Rather than gathering reaction force measurements from each of the 26 attachment points, data was collected at the corners and midspan of each side, resulting in data being collected at 14 points. Based on the results found by Wedding, it was shown that instrumenting these locations would still allow for accurate load distribution measurements while limiting the number of tests per BRGS. Limiting the number of tests conducted on a single polycarbonate sample is important as polycarbonate tends to build up residual stresses, which can have a negative effect on test results.

The BRGS samples tested were each 66 inches tall by 44.75 inches wide and of identical construction other than polycarbonate thickness. The first sample tested had a nominal polycarbonate thickness of 0.25 inches while the second sample had a nominal thickness of 0.50 inches. The samples were bonded to an extruded aluminum frame using structural glazing tape. This construction is consistent with the construction of the laminated glass sample tested previously. Figure 4.1 presents a cross-sectional view of the aluminum framing material along with the glazing tape.

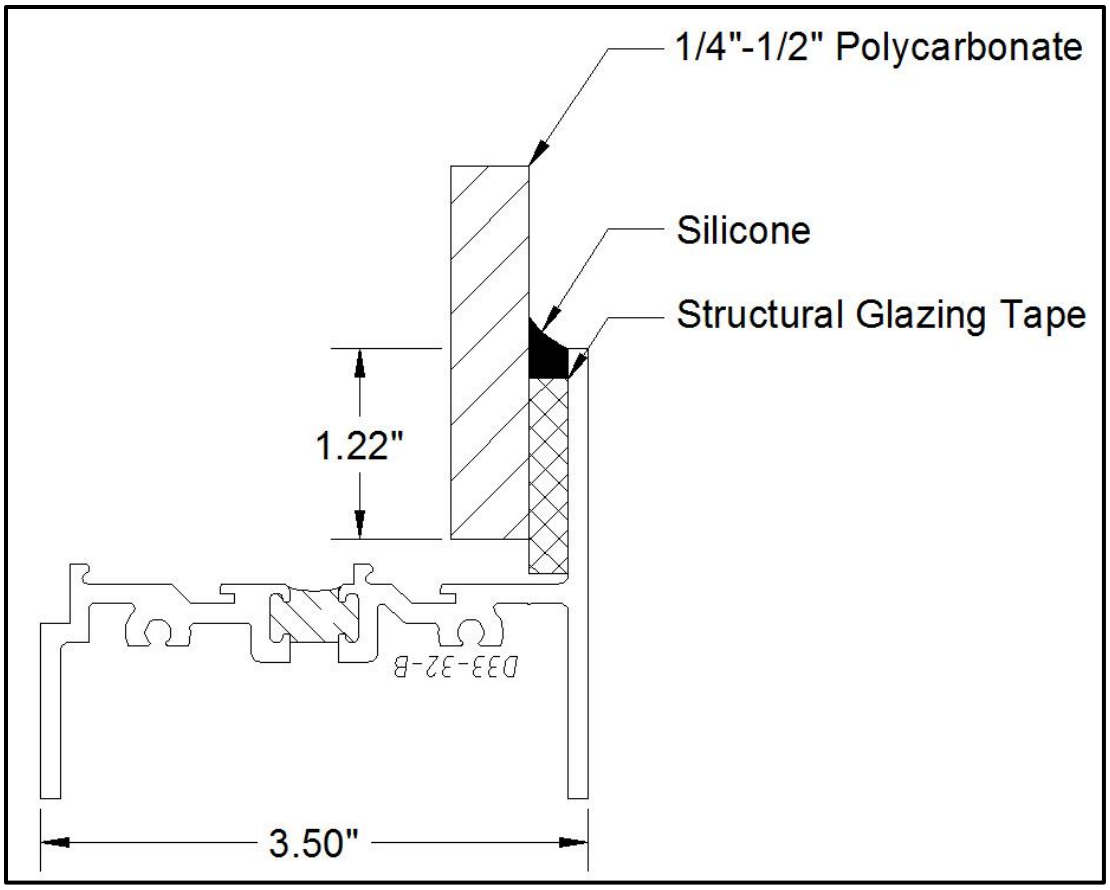

Figure 4.1: Cross sectional view of blast-resistant glazing system sample

The first phase of testing populated the 14 attachment points to characterize the load distribution at the corners and midpoints of each BRGS. During the second phase of testing, sensors were placed on either side of the window at midspan to determine the repeatability of the results and remain consistent with the methodology used in the laminated glass study. Finally, the charge size was increased until the point that the BRGS failed. This was done to determine the peak loading exerted by the system as it failed.

4.1 Explosives Standard Operating Procedure

Safety is of the utmost importance while handling explosive materials. Care was taken throughout the test series to ensure that the explosives used were handled in a safe and responsible manner. All applicable regulations were followed and the handling of explosives was conducted under the supervision of a licensed blaster.

For this test series, desensitized RDX Comp C-4 was used as the explosive product. C-4 was chosen due to its relative safety and ease of handling. Charges were weighed on an electronic balance to the nearest tenth of a gram. The product was then placed in a nitrile glove and formed into a spherical charge. A non-electric detonator was inserted into the charge and then hung inside the “cannon.” The cannon is a two foot diameter heavy gauge steel pipe centered vertically and horizontally within the shock tube. The cannon’s purpose is to direct the blast along the length of the shock tube and limit the damage to the shock tube walls in the area of the blast.

4.2 Perimeter Testing

The attachment points were assigned alphabetical labels starting in the lower left corner and proceeding around the perimeter in a clockwise fashion, lettered A through Z. Figure 4.2 shows the location of these points graphically as seen from outside the shocktube. Testing began with the load cells placed in positions A, D, E, and H to characterize the loading at the corners and mid-point of the left side of the glazing system. Three tests were completed in this configuration with a charge size of 175 grams at a standoff distance of 77 feet.

After the completion of these three tests the load cells were moved in a similar configuration to the top, right, and bottom sides. This allowed characterization of the corners and midpoints of all four sides of each BRGS over the course of 12 tests. The test configurations are referred to in the following manner.

- Setup 1 – positions A, D, E, and H populated
- Setup 2 – positions H, I, K, and M populated
- Setup 3 – positions N, Q, R, and U populated
- Setup 4 – positions U, V, X and Z populated

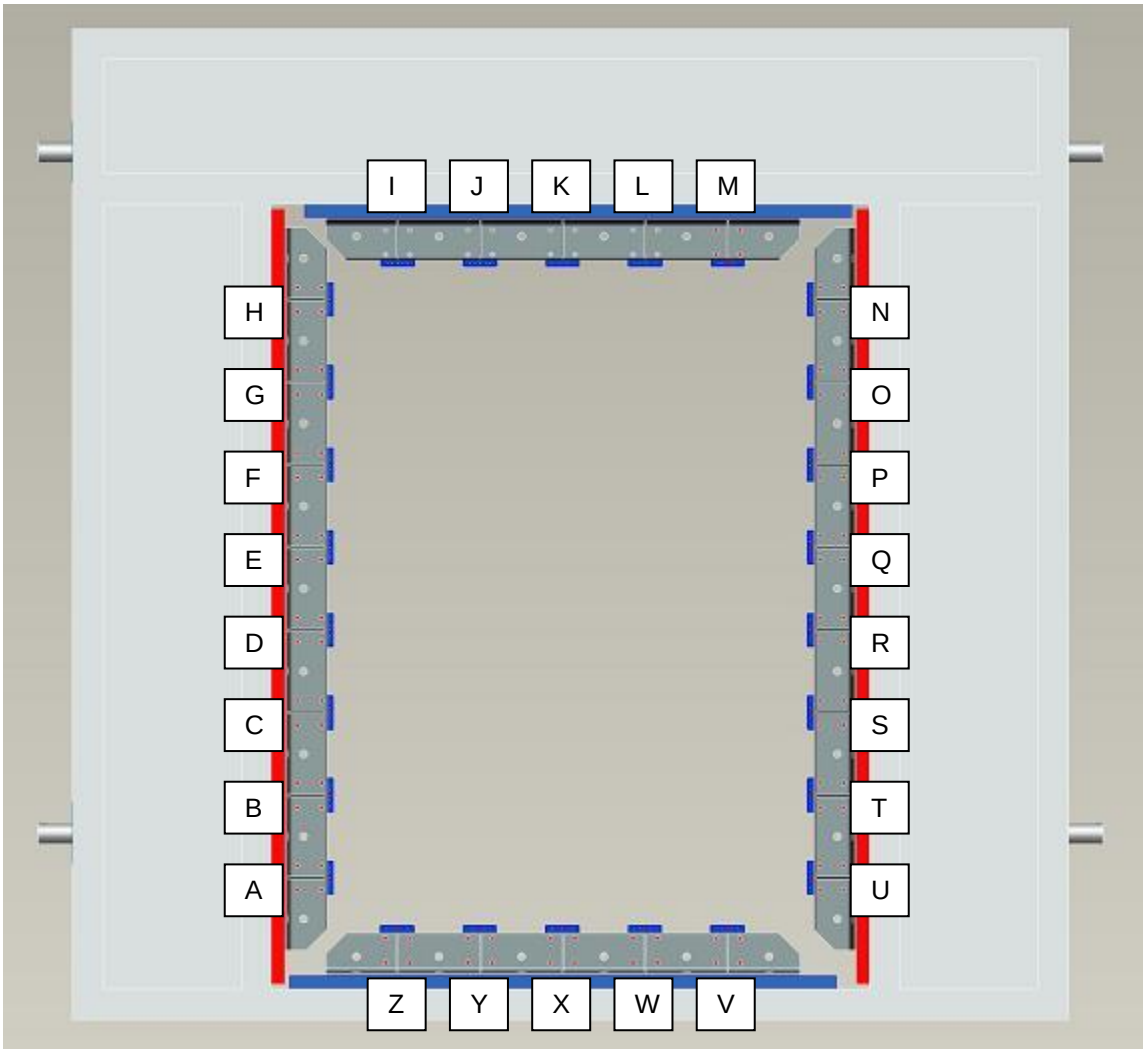

Figure 4.2: Attachment point labeling (Wedding, 2010)

4.3 Repeatability Testing

For repeatability testing the load cells were placed in positions D, E, Q, and R, referred to as Setup 5. These locations were chosen to remain consistent with the work completed by W.C. Wedding (Wedding, 2010) and because of the expectation that the reaction forces would be highest in these locations. The charge weight remained consistent at 175 grams and a standoff distance of 77 feet. Each BRGS was tested five times in this configuration.

4.4 Test to Failure

The final phase of testing for each polycarbonate blast-resistant glazing system was to test until the system failed. Since polycarbonate does not shatter like glass typically does, it was anticipated that the structural silicone glazing bond or aluminum framing material would likely fail first. For each sample, the cannon was left at a distance of 77 feet but the charge size was progressively increased until the system failed.

The 1/4” thick polycarbonate system required two shots to cause breakage. The first charge was 400 grams and the final charge was 600 grams. The screws holding the aluminum framing to the attachment points failed, allowing the glazing system to be sucked back into the shock tube during the negative phase.

The 1/2" thick polycarbonate system required three shots before finally failing. The first and second charges were 400 and 600 grams, respectively. With very limited visible damage to the framing material, it was decided to increase the charge size to 900 grams for the final test. The mode of failure was

consistent, with the screws failing and the glazing system being pulled back into the shock tube during the negative phase. After testing it was determined that the glazing system travelled 14 feet back into the shock tube, flipping many times in the process.

4.5 Supplemental Testing

After analysis of the data began for the first round of testing, it was discovered that one of the load cells had a faulty Z-axis that was providing irregular results. As a result, no usable data was collected for the Z-axis in the A, M, and U positions for the 1/4 inch and 1/2 inch polycarbonate samples. It was decided to conduct supplemental testing on an additional 1/2 inch polycarbonate sample to fill in the hole left by the previous test series. An additional 1/4 inch sample was not available for testing.

For this supplemental test series, the load cells were placed at the top and bottom of the vertical spans, in positions A, H, N, and U. A total of five tests were conducted with a charge size of 175 grams at a standoff distance of 77 feet. One change made to this test series was to use two screws per attachment point rather than one in the hopes that the interface between the load cells and the glazing system frame would become more rigid, providing cleaner reaction force results.

Chapter Five: Perimeter Testing Results and Analysis

5.1 Pressure Results

Pressure results were obtained using pressure sensors mounted on the left and right sides of the sample. The values from the two sensors were then averaged together. Pressure results and calculated impulses remained very consistent throughout the test series for both the 1/4 inch sample and 1/2 inch samples. The average pressure and impulse for the 1/4 inch test series was 4.657 psi and 20.336 psi-ms, respectively. The first 1/2 inch test series provided similar results with an average pressure of 4.744 psi and impulse of 20.990 psi-ms. The supplemental 1/2 inch test series presented an average maximum pressure of 4.885 psi and impulse of 20.320 psi-ms. A representative pressure time history graph is shown in Figure 5.1. This graph is from 1/4 Inch Polycarbonate Test 2. Test 2 of the 1/4 Inch test series exhibited a maximum pressure and impulse very close to the overall averages noticed throughout the perimeter test series.

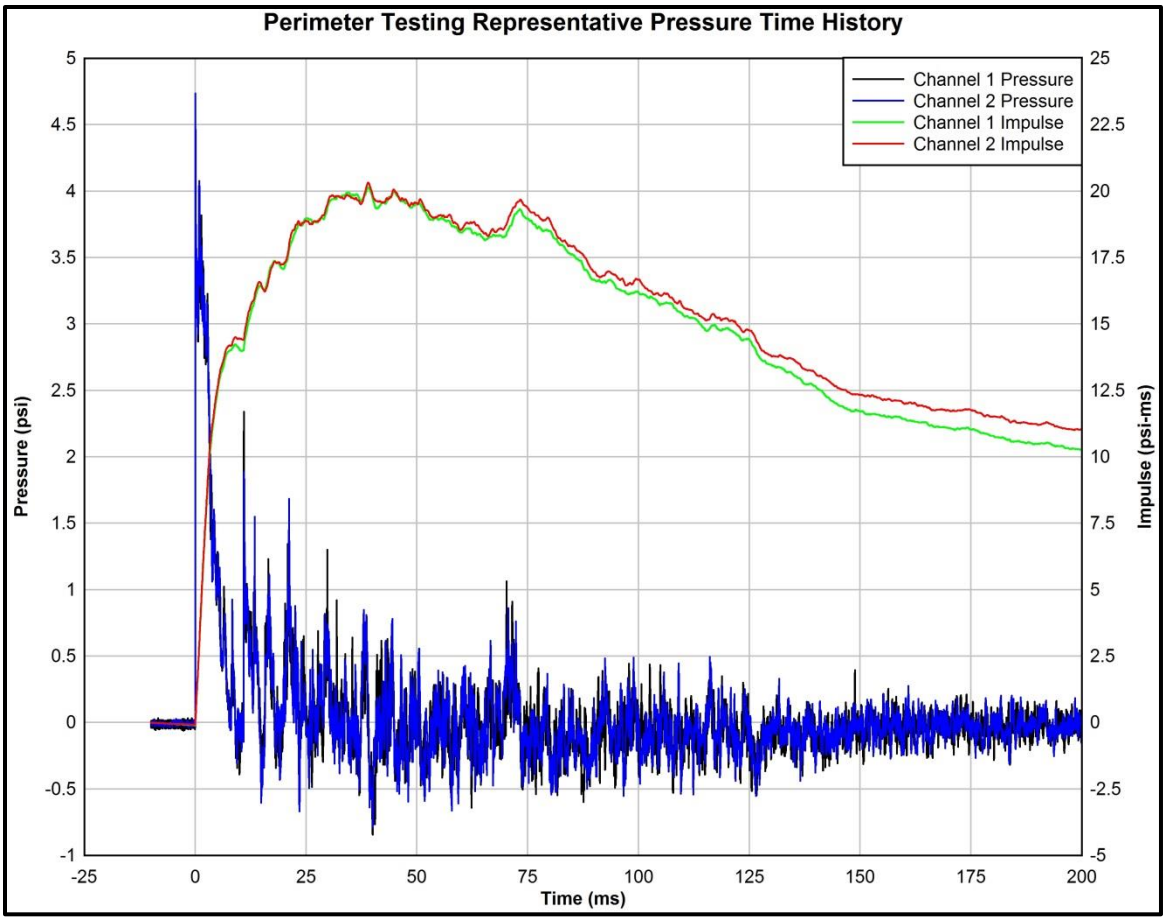

Figure 5.1: Perimeter Testing Representative Pressure Time History

Tables 5.1 through 5.3 summarize the peak pressure and impulses recorded during the 1/4 inch and 1/2 inch perimeter test series. It can be seen that there is minimal variance in the results. Across the three test series average peak pressure values ranged from 4.479 psi to 5.010 psi. Impulses ranged from 19.725 psi-ms to 22.068 psi-ms.

Table 5.1: 1/4 Inch Polycarbonate Peak Pressure and Impulse

Blast Event		Positive Phase Maximum Values					
System Type	Test #	Channel		Avg Peak Pressure (psi)	Channel		Avg Peak Impulse (psi-ms)
		1	2		1	2	
1/4 Poly	1	4.723	4.310	4.516	20.343	20.323	20.333
1/4 Poly	2	4.712	4.736	4.724	20.142	20.321	20.231
1/4 Poly	3	4.676	4.675	4.675	19.966	20.117	20.041
1/4 Poly	4	4.736	4.352	4.544	20.824	21.261	21.043
1/4 Poly	5	4.890	4.346	4.618	20.036	20.054	20.045
1/4 Poly	6	4.884	4.620	4.752	20.218	20.589	20.404
1/4 Poly	7	4.556	4.468	4.512	20.623	20.773	20.698
1/4 Poly	8	4.778	4.833	4.806	19.662	19.805	19.734
1/4 Poly	9	4.634	4.858	4.746	20.194	20.385	20.289
1/4 Poly	10	4.813	4.858	4.835	20.434	20.670	20.552
1/4 Poly	11	4.569	4.407	4.488	20.366	20.423	20.394
1/4 Poly	12	4.813	4.511	4.662	20.389	20.149	20.269
Average				4.657			20.336
Standard Deviation				0.120			0.335
Maximum				4.835			21.043
Minimum				4.488			19.734

Table 5.2: 1/2 Inch Polycarbonate Peak Pressure and Impulse

Blast Event		Positive Phase Maximum Values					
System Type	Test #	Channel		Avg Peak Pressure (psi)	Channel		Avg Peak Impulse (psi-ms)
		1	2		1	2	
1/2 Poly	1	4.676	5.029	4.852	20.631	20.848	20.740
1/2 Poly	2	4.879	4.925	4.902	20.338	20.323	20.330
1/2 Poly	3	4.807	4.797	4.802	20.422	20.581	20.502
1/2 Poly	4	5.010	5.010	5.010	21.882	22.020	21.951
1/2 Poly	5	4.569	4.389	4.479	20.223	20.203	20.213
1/2 Poly	6	4.712	5.016	4.864	19.933	19.824	19.879
1/2 Poly	7	4.867	5.083	4.975	20.941	21.462	21.202
1/2 Poly	8	4.569	4.401	4.485	20.598	21.032	20.815
1/2 Poly	9	4.581	4.663	4.622	20.731	21.198	20.965
1/2 Poly	10	4.700	4.773	4.736	21.280	21.701	21.490
1/2 Poly	11	4.778	4.541	4.659	21.575	21.881	21.728
1/2 Poly	12	4.676	4.413	4.544	21.768	22.369	22.068
Average				4.744			20.990
Standard Deviation				0.185			0.709
Maximum				5.010			22.068
Minimum				4.479			19.879

Table 5.3: 1/2 Inch Polycarbonate Supplemental Testing Peak Pressure and Impulse

Blast Event		Positive Phase Maximum Values					
System Type	Test #	Channel		Avg Peak	Channel		Avg Peak
		1	2	Pressure (psi)	1	2	Impulse (psi-ms)
1/2 Poly R2	1	4.838835	5.142857	4.991	20.20042	20.48055	20.340
1/2 Poly R2	2	4.594175	5.069444	4.832	21.32795	21.43655	21.382
1/2 Poly R2	3	4.939806	5.014881	4.977	20.30893	20.47745	20.393
1/2 Poly R2	4	4.493204	4.94721	4.720	19.57265	19.87767	19.725
1/2 Poly R2	5	4.802913	5.002976	4.903	19.6826	19.83712	19.760
Average				4.885			20.320
Standard Deviation				0.112			0.671
Maximum				4.991			21.382
Minimum				4.720			19.725

5.2 Deflection Results

Deflection results were obtained using the laser deflection gauge. Deflections away from the blast are recorded as negative deflections since the gauge is placed outside the shock tube. Deflection results presented by the 1/4 inch test series were consistent with minimal variability and are summarized in Table 5.4. The average deflection is -4.113 inches with a maximum deflection of -4.510 inches and a minimum deflection of -3.944 inches. The time of peak deflection varied from 9.8 ms to 10.5 ms. The graph from 1/4 inch polycarbonate test 4, found in Figure 5.2, shows a deflection time curve typical of the 1/4 inch test series.

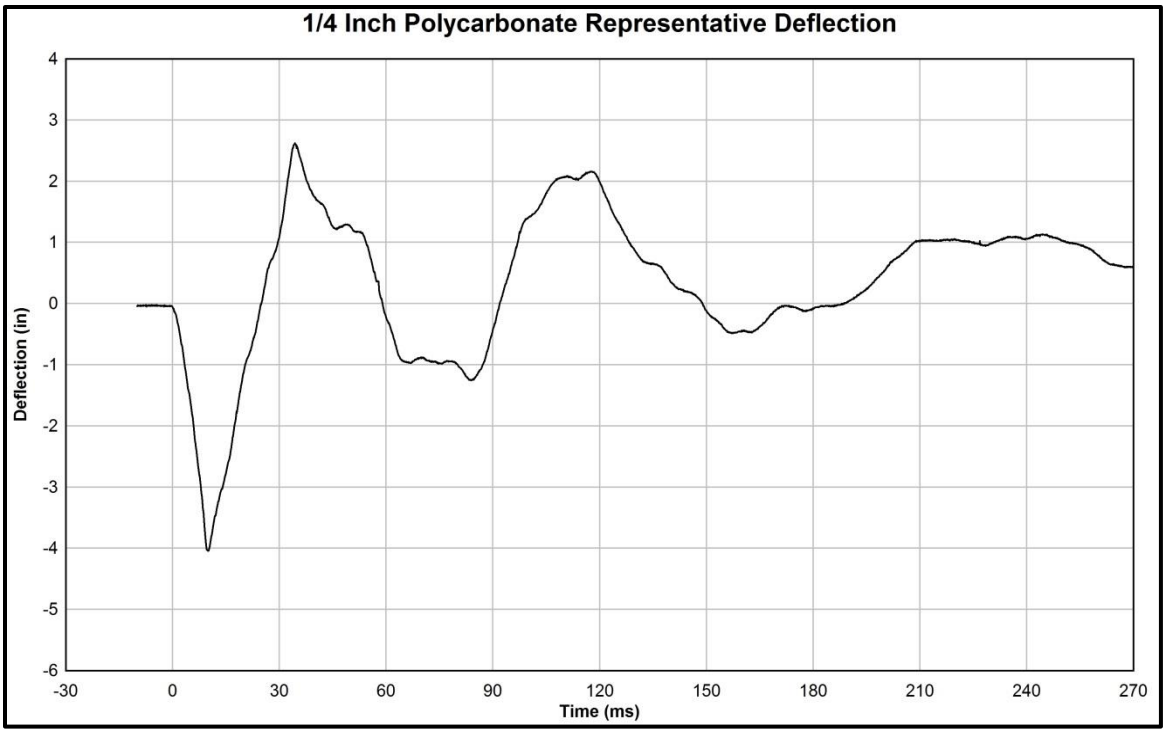

Figure 5.2: 1/4 Inch Polycarbonate Representative Deflection

Table 5.4: 1/4 Inch Polycarbonate Peak Deflection and Time

Blast Event		Peak Deflection	
System Type	Test #	Deflection (in)	Time (ms)
1/4" Poly	1	-4.081	9.9
1/4" Poly	2	-4.091	10.1
1/4" Poly	3	-4.144	10.0
1/4" Poly	4	-4.035	9.8
1/4" Poly	5	-4.110	10.0
1/4" Poly	6	-4.096	10.1
1/4" Poly	7	-3.944	9.9
1/4" Poly	8	-4.131	10.0
1/4" Poly	9	-4.147	10.1
1/4" Poly	10	-4.116	10.0
1/4" Poly	11	-4.510	10.5
1/4" Poly	12	-3.949	9.9
	Average	-4.113	10.03
	Standard Deviation	0.142	0.18
	Maximum	-4.510	10.50
	Minimum	-3.944	9.80

During the 1/2 inch test series, deflection results were not recorded for Setup 1. This was a result of improper instrument setup and was corrected for the following tests. Deflection results for the 1/2 inch test series were again very consistent with an average of -3.002 inches for the first test series and -3.034 for the supplemental test series. Table 5.5 summarizes the first test series and is followed by Table 5.6 summarizing the supplemental test series. Deflections varied from -2.846 inches to -3.085 inches. A representative graph of the 1/2 inch polycarbonate deflection is shown in Figure 5.3. This graph is from test 5 of the supplemental test series and is typical of the deflection response recorded for the other tests in the 1/2 inch polycarbonate tests.

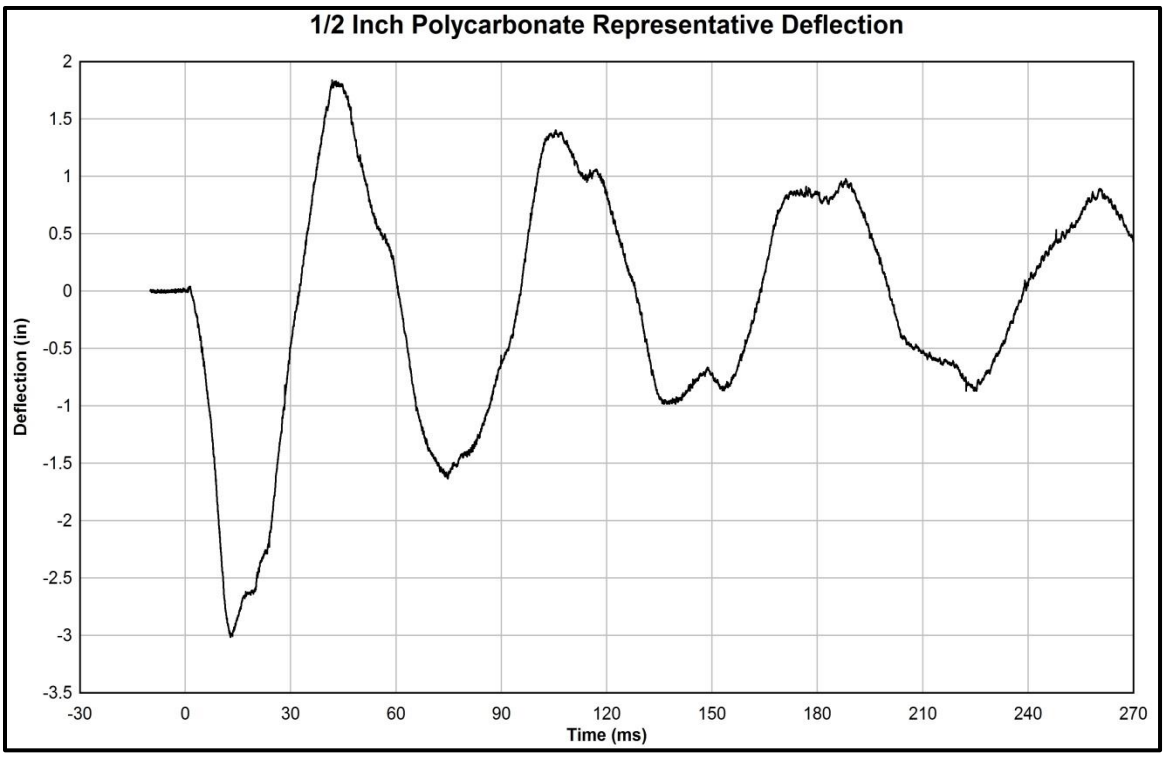

Figure 5.3: 1/2 Inch Polycarbonate Representative Deflection

Table 5.5: 1/2 Inch Polycarbonate Peak Deflection and Time

Blast Event		Peak Deflection	
System Type	Test #	Deflection (in)	Time (ms)
1/2" Poly	1	-	-
1/2" Poly	2	-	-
1/2" Poly	3	-	-
1/2" Poly	4	-3.014	11.9
1/2" Poly	5	-3.021	12.3
1/2" Poly	6	-3.085	12.7
1/2" Poly	7	-2.846	11.9
1/2" Poly	8	-2.890	12.3
1/2" Poly	9	-3.067	12.4
1/2" Poly	10	-3.031	12.4
1/2" Poly	11	-3.022	12.5
1/2" Poly	12	-3.040	12.7
Average		-3.002	12.34
Standard Deviation		0.080	0.29
Maximum		-3.085	12.70
Minimum		-2.846	11.90

Table 5.6: 1/2 Inch Polycarbonate Supplemental Testing Peak Deflection and Time

Blast Event		Peak Deflection	
System Type	Test #	Deflection (in)	Time (ms)
1/2" Poly R2	1	-3.018	12.7
1/2" Poly R2	2	-3.071	12.8
1/2" Poly R2	3	-3.059	13.0
1/2" Poly R2	4	-3.007	13.2
1/2" Poly R2	5	-3.014	12.9
Average		-3.034	12.90
Standard Deviation		0.029	0.19
Maximum		-3.071	13.20
Minimum		-3.007	12.70

Following the perimeter tests, each sample was measured to look for residual deformation of the polycarbonate. Residual deformation was noted at the end of the test series for the 1/4 inch polycarbonate, however, the 1/2 inch polycarbonate showed no signs of deformation. The deformation was approximately 0.75 inches and is shown in Figure 5.4 below. Deformation was measured by placing a straightedge across the midspan of the window and measuring the difference between the straightedge and the polycarbonate.

Figure 5.4: Residual deflection of 1/4 inch polycarbonate after perimeter testing.

5.3 Reaction Results – Z-Axis

As stated previously, reaction force data collection posed somewhat of a challenge. The results presented by the reaction measurements are less consistent and feature a number of anomalies when compared to pressure and

deflection results. Although the results are not as clear, some general patterns can still be observed and will be discussed in the following sections. This section, and a majority of the remainder of this thesis, will focus on the Z-axis reactions. However, some points will be made regarding the X and Y axes in future sections; particularly the X axis on the long edges and the Y axis on the short edges as these forces are significant in many cases.

A major challenge presented during the Z-axis analysis was the result of faulty instrumentation. One of the four triaxial load cells produced erroneous results on its Z-axis. These errors consisted of many large voltage spikes and drops that did not correspond with the blast event. This error went unnoticed until after the test series was completed and data analysis began. Z-axis data from this load cell could not be salvaged. Therefore, for both the quarter inch and half inch samples, Z-axis data was not available for positions A, M, and U. Supplemental testing was done in an attempt to fill in these holes and will be discussed in the Half Inch Polycarbonate section, 5.3.2.

5.3.1 Quarter Inch Polycarbonate

The first sample tested was the 1/4 inch polycarbonate blast resistant glazing system. As this was the research team's first time instrumenting a polycarbonate panel in this manner, a number of uncertainties were presented which ultimately led to some errors that may have affected the data. The most notable mishap occurred on Test 11. A number of screws pulled out of the framing material and allowed the glazing system to partially fall from the attachment points. The glazing system was reattached to the attachment points

and following each remaining test the screws were checked for tightness and repositioned if pullout appeared imminent. This appeared to have very little effect on the peak Z-axis loading for the test in question.

Upon first examination of the Z-axis data gathered during perimeter testing of the 1/4 inch polycarbonate, the data appears to be rather inconsistent. However, after closer examination, some patterns begin to appear. A summary of the maximum positive Z-axis loading is presented below in Table 5.7. For this report, negative Z-axis loading will not be analyzed. The long edges (sides) are shown in white and the short edges (top and bottom) are highlighted in blue.

Table 5.7: Summary of 1/4 inch polycarbonate peak positive Z-axis loading

1/4 Inch Polycarbonate Perimeter Testing								
	Maximum Positive Z- Axis Loading							
Position	Test #	Force (lbf)	Test #	Force (lbf)	Test #	Force (lbf)	Avg Force (lbf)	Avg Force per Edge (lbf)
A	1	-	2	-	3	-	-	642.37
D	1	297.26	2	327.63	3	318.22	314.37	
E	1	406.13	2	490.85	3	420.18	439.05	
H	1	1206.95	2	1199.00	3	1164.64	1173.69	
H	4	1104.97	5	1200.67	6	1165.90		
I	4	569.18	5	617.71	6	617.71	601.53	416.05
K	4	219.95	5	226.69	6	245.08	230.57	
M	4	-	5	-	6	-	-	
N	7	1110.49	8	1134.90	9	1170.93	1138.77	638.16
Q	7	336.74	8	420.18	9	447.85	401.59	
R	7	375.96	8	361.42	9	384.94	374.11	
U	7	-	8	-	9	-	-	
U	10	-	11	-	12	-	-	
V	10	260.48	11	491.02	12	363.99	371.83	260.31
X	10	234.99	11	216.69	12	247.77	233.15	
Z	10	171.76	11	181.82	12	174.28	175.95	

Looking at each position individually, the first pattern realized is the distribution of loads along the long edges, in positions A-H and positions N-U. The loading appears to be greatest at the top in positions H and N, and decrease as it continues towards the midpoint. The peak loadings are 1173.69 lbf at position H and 1138.77 lbf at position N. The long side cannot be fully characterized as data is not available for positions A and U, but it is assumed that these positions would exhibit loadings similar to that of the top, approximately 1100 lbf. The next pattern becomes distinguishable after the loads for each edge are averaged. Of particular interest is the fact that the average loading of the left and right sides differ by only 4.21 lbf, or less than 1%. A greater difference is noticed between the top and bottom edges, with the top edge average force equaling 416.05 lbf and the bottom edge equaling 260.31 lbf. The bottom edge force is approximately 62% of the top edge force. Currently, no pattern may be evident regarding the top and bottom edges, but following the analysis of the Z-axis data for the 1/2 inch polycarbonate, some similarities will be shown.

5.3.2 Half Inch Polycarbonate

Following the lessons learned from the 1/4 inch testing, screws at the 26 attachment points were checked following each test of the 1/2 inch polycarbonate. No major mishaps were observed, other than the single faulty Z-axis. One unexplained concern did arise following the analysis of the data on Test 9. For an unknown reason, the peak loading experience by position N on this test was dramatically lower than the previous two tests at that position.

Loads experience by positions Q and R were higher than previously recorded. For analysis, the values recorded on Test 9 are not used. A summary of values recorded for 1/2 inch polycarbonate perimeter testing are shown in Table 5.8 with long edge values in white and short edge values highlighted in blue. The unused values of test 9 are highlighted in red font.

Table 5.8: Summary of 1/2 inch polycarbonate peak positive Z-axis loading

1/2 Inch Polycarbonate Perimeter Testing								
	Maximum Positive Z- Axis Loading							
Position	Test #	Force (lbf)	Test #	Force (lbf)	Test #	Force (lbf)	Avg Force (lbf)	Avg Force per Edge (lbf)
A	1	-	2	-	3	-	-	537.53
D	1	361.42	2	357.57	3	361.42	360.14	
E	1	249.04	2	289.48	3	323.54	287.35	
H	1	847.93	2	976.54	3	958.53	965.09	
H	4	1055.30	5	989.53	6	962.71		
I	4	429.54	5	466.16	6	488.29	461.33	366.47
K	4	264.76	5	272.46	6	277.59	271.60	
M	4	-	5	-	6	-	-	
N	7	993.30	8	794.30	9	345.20	893.80	537.80
Q	7	469.99	8	446.57	9	522.35	458.28	
R	7	264.76	8	257.91	9	382.38	261.33	
U	7	-	8	-	9	-	-	
U	10	-	11	-	12	-	-	
V	10	293.75	11	226.20	12	275.37	265.11	212.63
X	10	256.78	11	239.32	12	233.12	243.07	
Z	10	142.15	11	129.06	12	117.92	129.71	

Similar to the 1/4 inch data, the first pattern noticed when looking at the 1/2 inch data, is the distribution of forces along the long edges. The peak loadings were recorded at positions H and N, with values of 965.09 lbf and 893.80 lbf, respectively. One outlier in the distribution of loading on the long edges is observed at positions D and E, with position D exhibiting a higher

loading than E. However, loadings on the opposite side, positions N-R show greater loadings at the top and decreasing loads towards the lower midpoint position. Again, the long edges cannot be fully characterized due to the lack of data in positions A and U.

A very noticeable similarity occurs when the loadings along each edge are averaged. The left and right sides have nearly identical loadings with values of 537.53 lbf and 537.80 lbf, respectively. The top and bottom edges differ by 153.84 lbf or 58%, similar to the 62% noticed on the 1/4 inch sample.

As mentioned previously, data was not recorded at the lower most positions on the long edges. Therefore, a simple supplemental test series involving five tests was conducted to try to fill in these holes. Load cells were placed in the lower and upper most positions on both long edges. Although the results were not definitive, a better idea of what is occurring can be observed from these results. A summary of the supplemental test series is shown in Table 5.9. To prevent skewing of data, the results from the supplemental testing are not combined with the original perimeter testing.

Some assumptions based on the data can be made, but saying the results are definitive would not be justified at this time. It is noted that the values recorded for right side positions N and U are within 10% of each other. However, the values recorded on the left side in positions H and A differ by approximately 60%. Based on this information, the only conclusion that the author feels safe stating is that the values observed at the top and bottom of the long edges are likely higher than those observed at the mid span.

Table 5.9: Summary of 1/2 inch polycarbonate peak positive Z-axis loading during supplemental perimeter testing

1/2 Inch Polycarbonate Perimeter Testing - Supplemental											
	Maximum Positive Z- Axis Loading										
Position	Test #	Force (lbf)	Test #	Force (lbf)	Test #	Force (lbf)	Test #	Force (lbf)	Test #	Force (lbf)	Avg Force (lbf)
A	1	1128.26	2	1272.80	3	1207.25	4	1206.03	5	1223.53	1208.20
D											
E											
H	1	707.61	2	732.58	3	722.51	4	745.87	5	745.87	728.69
H											
I											
K											
M											
N	1	1026.62	2	1043.97	3	1029.04	4	1011.70	5	990.72	1020.44
Q											
R											
U	1	868.44	2	963.83	3	936.80	4	949.13	5	943.96	925.41
U											
V											
X											
Z											

5.4 Comparison of Z-axis Reaction Results

When comparing the reaction forces of the polycarbonate panels side by side, interesting and possibly very important patterns emerges. The most notable of these differences is that the magnitude of Z-axis loading is less for the 1/2 inch polycarbonate when compared to the 1/4 inch polycarbonate. Next, the average reaction force for each of the edges was compared to the average reaction force of the left edge and expressed as a percentage. This comparison is shown in Table 5.10. Following the table in Figures 5.5 and 5.6 are graphical representations of the load distributions for the 1/4 inch and 1/2 inch samples.

From this comparison, it can be seen that on a percentage basis, the load distributions for each of the sides is very similar between the polycarbonate samples. This may indicate that it is possible to determine the load distribution

round the entire perimeter of a polycarbonate sample by instrumenting only one side.

Table 5.10: Comparison of load distribution

	1/4 Inch Poly			1/2 Inch Poly	
	Avg Force per Edge (lbf)	% of Left Side		% of Left Side	Avg Force per Edge (lbf)
Left Side	642.37	100.00		100.00	537.53
Top	416.05	64.77		68.18	366.47
Right Side	638.16	99.34		100.05	537.80
Bottom	260.31	40.52		39.56	212.63

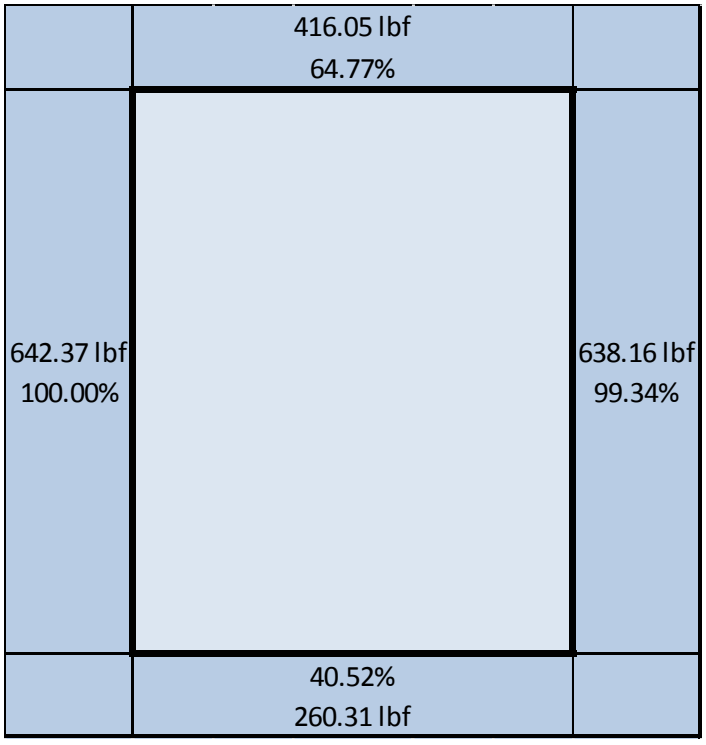

Figure 5.5: Load distribution for 1/4 inch polycarbonate

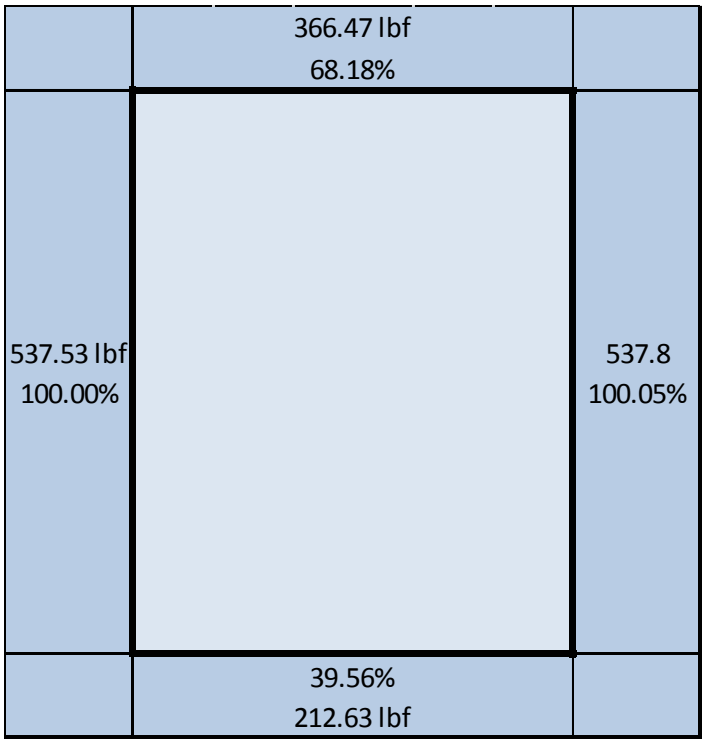

Figure 5.6: Load distribution of 1/2 inch polycarbonate

5.5 Reaction Results – X and Y Axes

The data recorded from the X and Y axes during perimeter testing of the 1/4 inch and 1/2 inch polycarbonate blast resistant glazing systems presented some interesting results. Generally, the loading from these axes is ignored. However, the author felt it important to highlight the trends present in the data given the magnitude of the loadings can be equal to or greater than those present in the Z-axis. For this discussion, the X-axis on the left and right side of the glazing systems will be evaluated. The Y-axis will be evaluated on the top and bottom edges. This methodology was chosen because the loading in these directions was generally greatest and may induce shear or bending moments. Axial loading is less of a concern.

5.5.1 Quarter Inch Polycarbonate

Data from the X and Y axes was recorded over the course of 12 tests. On Test 7, data was not recorded for position R_x due to a damaged cable. A summary of the data collected over the 12 perimeter tests is shown in Table 5.11. The left and right sides are white and the top and bottom edges are highlighted in blue. As stated previously, the values presented for the left and right side are X-axis values, and the top and bottom edges are Y-axis values. Positive values indicate tensile forces acting towards the center of the glazing system, while negative values indicate forces acting outwards, away from the center. A graphical representation of the average values for each position can be found in Figure 5.7. In this figure, the values are placed in the approximate location of where the load cells were placed during testing.

An anomaly present in the data can be found in Test 11, position V. This record indicates a maximum Y-axis loading of 404.44 lbf, while the other two test records in this position indicate loadings that are approximately half this value. The loading recorded for position X from test 11 also differs significantly from the values present in the other two test records. Therefore, these values are not included in the average for their positions and are highlighted in red.

Some interesting trends become apparent while looking at the data, especially along the long edges of the glazing system. The peak X-axis loadings can be found at the midpoints of the edges. At positions D and E, the values are -1364.55 lbf and -1310.15 lbf, respectively. Positions Q and R present values of -1038.81 lbf and -1027.31 lbf, respectively. Also of significance is the forces are

acting outward, away from the center of the window. This was not expected. The top and bottom corners have peak forces acting towards the center of the window, with values ranging from 627.01 lbf to 780.27, approximately half the magnitude of the values recorded at the midpoints.

The values recorded at the midpoint of the top and bottom edges are also significantly higher than the values recorded at the corners. In both cases, the forces are acting away from the center of the window. The direction of the peak values at the corners of the top and bottom edges varied and in most cases the magnitude of the positive and negative differed by less than 10%. To remain consistent, the peak values are listed in Table 5.11 and shown in Figure 5.7.

Table 5.11: Summary of X and Y axis data for 1/4 inch polycarbonate

1/4 Inch Polycarbonate Perimeter Testing							
Blast Event	Tension/Compression Loading						
Position	Test #	Force (lbf)	Test #	Force (lbf)	Test #	Force (lbf)	Avg Force (lbf)
A	1	672.6307	2	601.8791	3	641.9935	638.83
D	1	-1415.11	2	-1382.26	3	-1296.26	-1364.55
E	1	-1366.33	2	-1295.31	3	-1268.81	-1310.15
H	1	782.3529	2	793.8725	3	723.2026	780.27
H	4	750.2451	5	836.0294	6	795.915	
I	4	273.9314	5	252.0995	6	232.6131	252.88
K	4	-574.292	5	-686.571	6	-595.072	-618.64
M	4	-382.843	5	-392.811	6	-344.69	-373.45
N	7	644.8372	8	601.7974	9	634.3954	627.01
Q	7	-997.309	8	-1073.3	9	-1045.82	-1038.81
R	7	-	8	-1055.11	9	-999.507	-1027.31
U	7	553.268	8	724.2647	9	726.7157	729.83
U	10	893.7092	11	545.2614	12	935.7843	
V	10	200.7392	11	404.4353	12	202.2177	201.48
X	10	768.3653	11	587.8516	12	759.3151	763.84
Z	10	215.6863	11	249.2647	12	313.4804	264.58

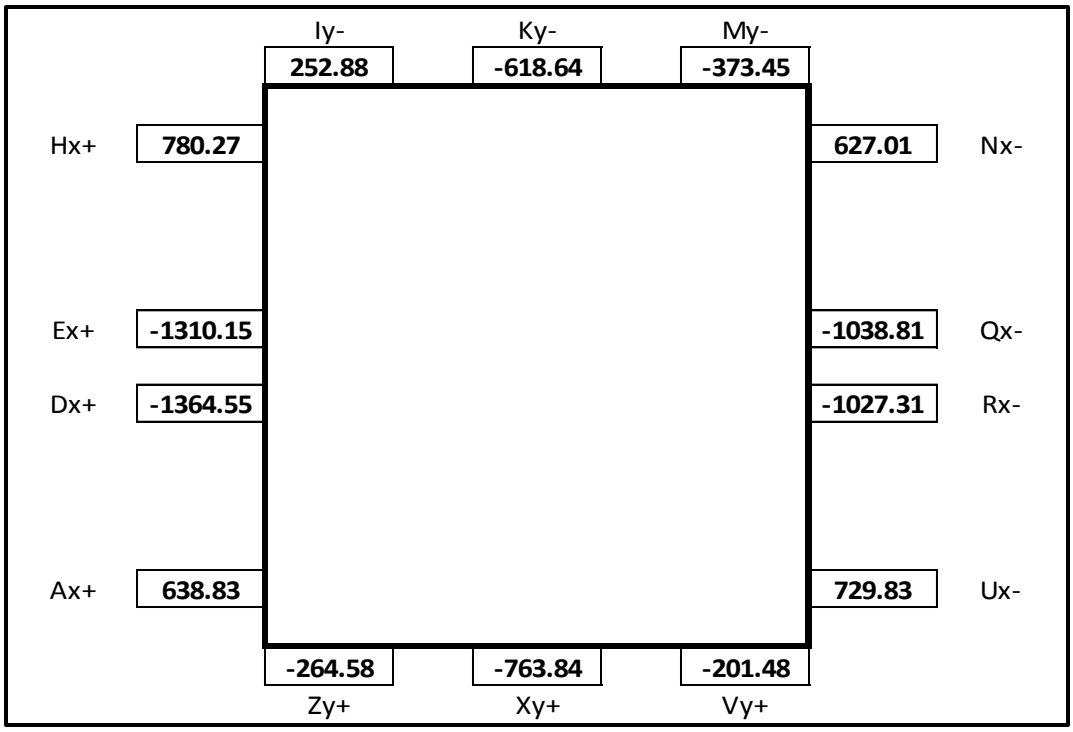

Figure 5.7: Load Distribution for 1/4 Inch Polycarbonate

5.5.2 Half Inch Polycarbonate

Data for the X and Y axes of the 1/2 inch polycarbonate presented many of the same patterns observed with the 1/4 inch polycarbonate with some key differences that will be discussed shortly. A summary of the results can be found in Table 5.12 with a graphical representation following in Figure 5.8. The number convention remains consistent with the previous section, with positive numbers acting towards the center of the window and negative numbers acting outward.

As before, the midpoints of the long edges experience peak loading acting away from the center of the glazing system. The key difference is the magnitude of the loading which is observed to be roughly half of that noticed with the 1/4 inch polycarbonate system. Peak loadings are instead found at the bottom corners of the long edges with the left side experiencing a peak force of 791.26

lbf at position A and the right side experiencing a peak force of 777.908 lbf at position U.

The greatest loadings for the top and bottom edges were again found at the midpoint, acting away from the center of the glazing system. The direction and magnitude of the peak loadings for the corners varied. As with the 1/4 inch polycarbonate, the difference in magnitude between positive peak loading and negative peak loading generally did not exceed 10%. The maximum magnitude is reported to remain consistent with the data presented for the long edges.

Table 5.12: Summary of X and Y axis data for 1/2 inch polycarbonate

1/2 Inch Polycarbonate Perimeter Testing							
Blast Event	Tension/Compression Loading						
Position	Test #	Force (lbf)	Test #	Force (lbf)	Test #	Force (lbf)	Avg Force (lbf)
A	1	827.5327	2	742.3203	3	803.9216	791.26
D	1	-694.127	2	-570.267	3	-523.285	-595.89
E	1	-529.882	2	-601.875	3	-619.323	-583.69
H	1	469.9346	2	467.402	3	354.085	492.57
H	4	688.5621	5	543.6275	6	431.781	
I	4	278.1074	5	283.0819	6	316.1027	292.43
K	4	-507.105	5	-480.329	6	-500.534	-495.99
M	4	-395.343	5	-402.86	6	-422.386	-406.86
N	7	449.8366	8	405.2288	9	323.4477	392.8377
Q	7	-478.353	8	-526.376	9	-646.311	-550.347
R	7	-585.462	8	-622.341	9	-638.522	-615.442
U	7	708.1566	8	788.3987	9	797.4673	777.908
U	10	795.0755	11	828.0229	12	750.3268	
V	10	-190.062	11	-287.639	12	-318.029	-265.24
X	10	-477.607	11	-447.86	12	-470.363	-465.28
Z	10	187.5817	11	209.1503	12	202.6144	199.78

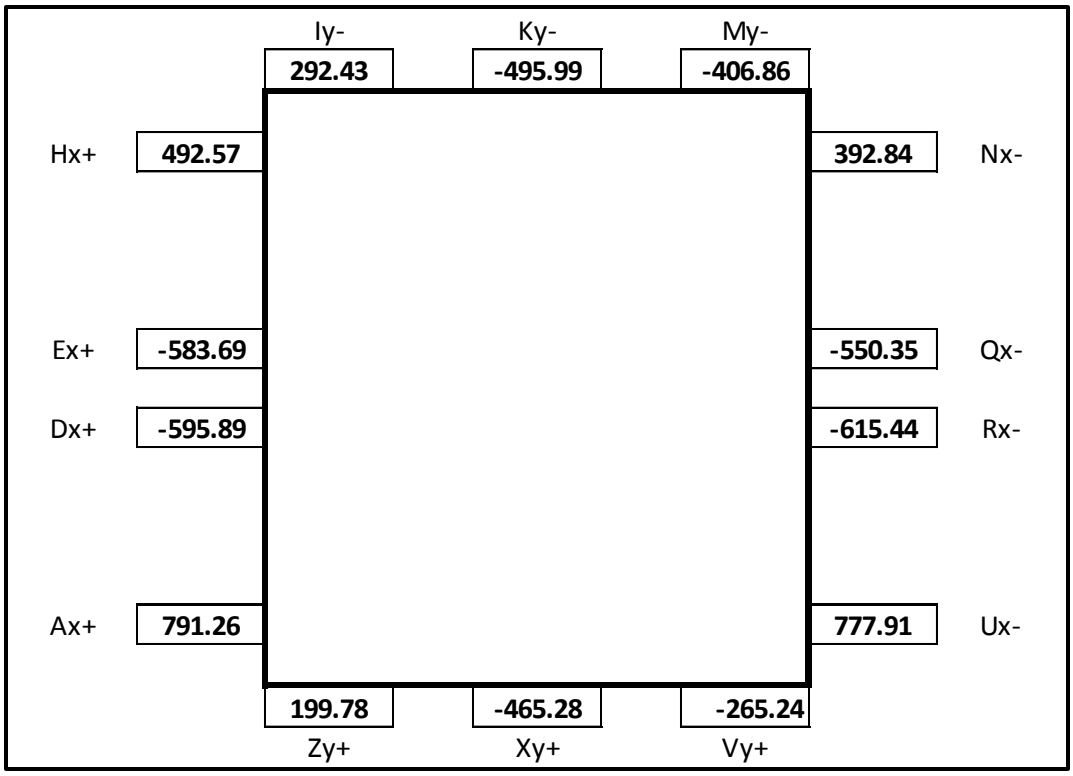

Figure 5.8: Load Distribution for 1/2 Inch Polycarbonate

Chapter Six: Repeatability Testing Results and Analysis

6.1 Pressure Results

Using the same charge size and standoff distance as used in perimeter testing, pressure results remained consistent throughout the repeatability test series. As with the perimeter test results, the differences between the recorded pressures of the two channels is negligible. A representative pressure time history is shown in Figure 6.1. This graph is from 1/2 Inch Polycarbonate Repeatability Test 3 and is characteristic of the pressures and impulses recorded throughout the test series.

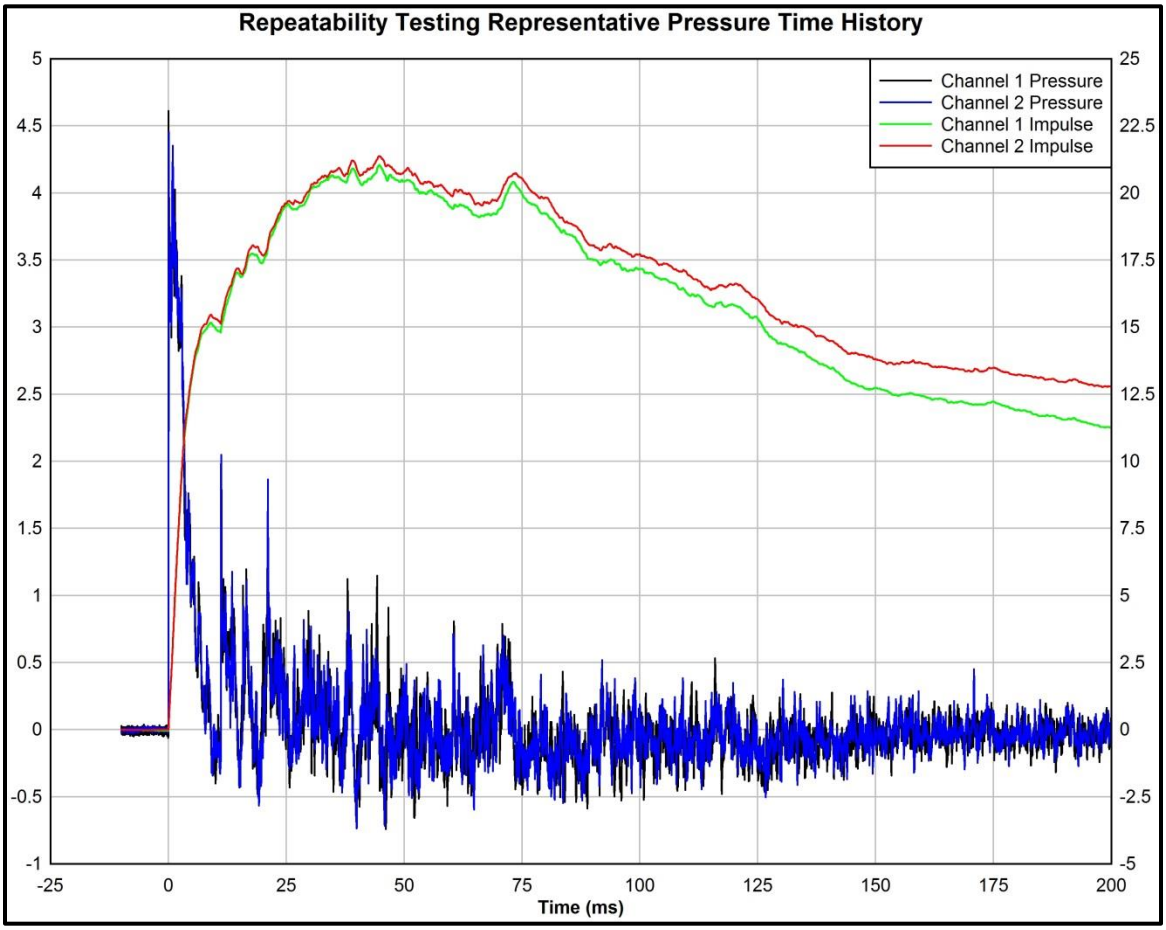

Figure 6.1: Repeatability Testing Representative Pressure Time History

During the 1/4 inch polycarbonate testing, the average peak pressure and impulse was 4.721 psi and 20.456 psi-ms, respectively. The average peak pressures ranged from 4.608 psi to 4.790 psi while the average peak impulses ranged from 20.009 psi-ms to 21.395 psi-ms, well within an acceptable range of 5% variation. The pressure and impulse results from the five repeatability tests are shown in the Table 6.1.

Table 6.1: 1/4 Inch Polycarbonate Repeatability Testing Peak Pressure and Impulse

Blast Event		Positive Phase Maximum Values					
System Type	Test #	Channel		Avg Peak Pressure (psi)	Channel		Avg Peak Impulse (psi-ms)
		1	2		1	2	
1/4 Poly	1	4.770874	4.809524	4.790	19.98729	20.0312	20.009
1/4 Poly	2	4.860194	4.631944	4.746	20.16743	20.30062	20.234
1/4 Poly	3	4.723301	4.492063	4.608	20.23134	20.36491	20.298
1/4 Poly	4	4.825243	4.559524	4.692	20.29375	20.39201	20.343
1/4 Poly	5	4.633981	4.900794	4.767	21.41213	21.3782	21.395
Average				4.721			20.456
Standard Deviation				0.073			0.541
Maximum				4.790			21.395
Minimum				4.608			20.009

As with the previous tests, the average peak pressures and impulses recorded during the 1/2 inch polycarbonate repeatability test remained consistent. The average peak pressure for the five tests was 4.723 psi. The average peak impulse was 21.364 psi-ms. Pressures ranged from 4.533 psi to 4.839 psi. Impulses ranged from 21.018 psi-ms to 21.976 psi-ms. Table 6.2 summarizes the results from the five repeatability tests.

Table 6.2: 1/2 Inch Polycarbonate Repeatability Testing Peak Pressure and Impulse

Blast Event		Positive Phase Maximum Values					
System Type	Test #	Channel		Avg Peak Pressure (psi)	Channel		Avg Peak Impulse (psi-ms)
		1	2		1	2	
1/2 Poly	1	4.717476	4.96131	4.839	21.92706	22.02505	21.976
1/2 Poly	2	4.664078	4.906746	4.785	20.96854	21.06791	21.018
1/2 Poly	3	4.61068	4.455357	4.533	21.05091	21.37716	21.214
1/2 Poly	4	4.753398	4.662698	4.708	21.39922	21.7249	21.562
1/2 Poly	5	4.675728	4.821429	4.749	20.80727	21.29226	21.050
Average				4.723			21.364
Standard Deviation				0.117			0.405
Maximum				4.839			21.976
Minimum				4.533			21.018

6.2 Deflection Results

The deflection results remained fairly consistent throughout the test series with one interesting exception. On Tests 1 and 5 of the 1/4 inch polycarbonate repeatability testing, peak deflection and corresponding time was noticeably lower. Upon examination of the deflection time curve, it was noticed that Tests 1 and 5 failed to develop an additional spike that was apparent in Tests 2 through 4. The root cause of this is unknown. A graphical comparison of the deflection is shown in Figure 6.2 with the lesser deflection shown in black and the greater deflection of Tests 2-5 shown in green. The lesser peak deflection in Tests 1 and 5 occurred at a time of approximately 10.0 ms and peaked at -3.733 inches and -3.921 inches, respectively. The remainder of the three tests had peak values averaging -4.513 inches at a time of 12.5 ms. The deflection results from the five tests are summarized in Table 6.3.

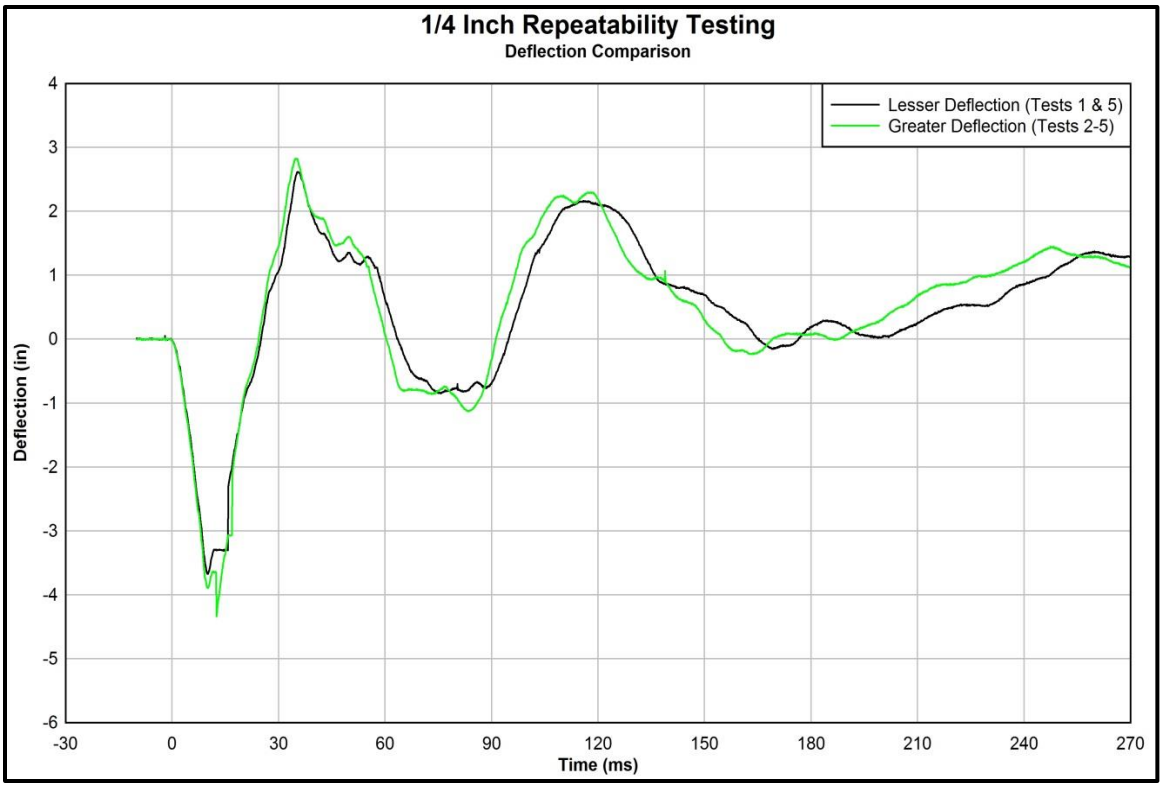

Figure 6.2: 1/4 Inch Polycarbonate Deflection Comparison

Table 6.3: 1/4 Inch Polycarbonate Repeatability Testing Peak Deflection and Time

Blast Event		Peak Deflection	
System Type	Test #	Deflection (in)	Time (ms)
1/4" Poly	1	-3.733	9.9
1/4" Poly	2	-4.409	12.5
1/4" Poly	3	-4.531	12.5
1/4" Poly	4	-4.600	12.6
1/4" Poly	5	-3.921	10.0
Average		-4.239	11.50
Standard Deviation		0.388	1.42
Maximum		-4.600	12.60
Minimum		-3.733	9.90

Following the five repeatability tests, the residual deformation of the 1/4 inch polycarbonate increased a noticeable amount. Using the same

measurement method as noted previously in Section 5.2, the residual deformation increased from 0.75 inches to approximately 1.25 inches as shown in Figure 6.3. An increase of 0.50 inches in residual deformation over a course of five tests could indicate that the polycarbonate was beginning to weaken and lose some of its elasticity. After a total of 17 tests, this was anticipated. It is well known that polycarbonate does not behave in a linear-elastic manner like that of laminated glass and may store residual stresses. This shows that the current test methodology may not appropriate and characterization of the polycarbonate should be conducted using the fewest number of tests practical.

Figure 6.3: Residual deformation of 1/4 inch polycarbonate following repeatability testing.

The peak deflection and recorded time for peak deflection remained very constant for the 1/2 inch polycarbonate during repeatability testing. Deflections ranged between -3.038 inches and -3.069 inches with an average of -3.055 inches. The time of peak deflection ranged from 12.3 ms to 12.6 ms. A graph showing a typical deflection time curve can be found in Figure 6.4. This graph is from ½ Polycarbonate Repeatability Test 3. A summary of the peak deflections can be found in Table 6.4. Following repeatability testing, there was no noticeable residual deformation of the 1/2 inch sample.

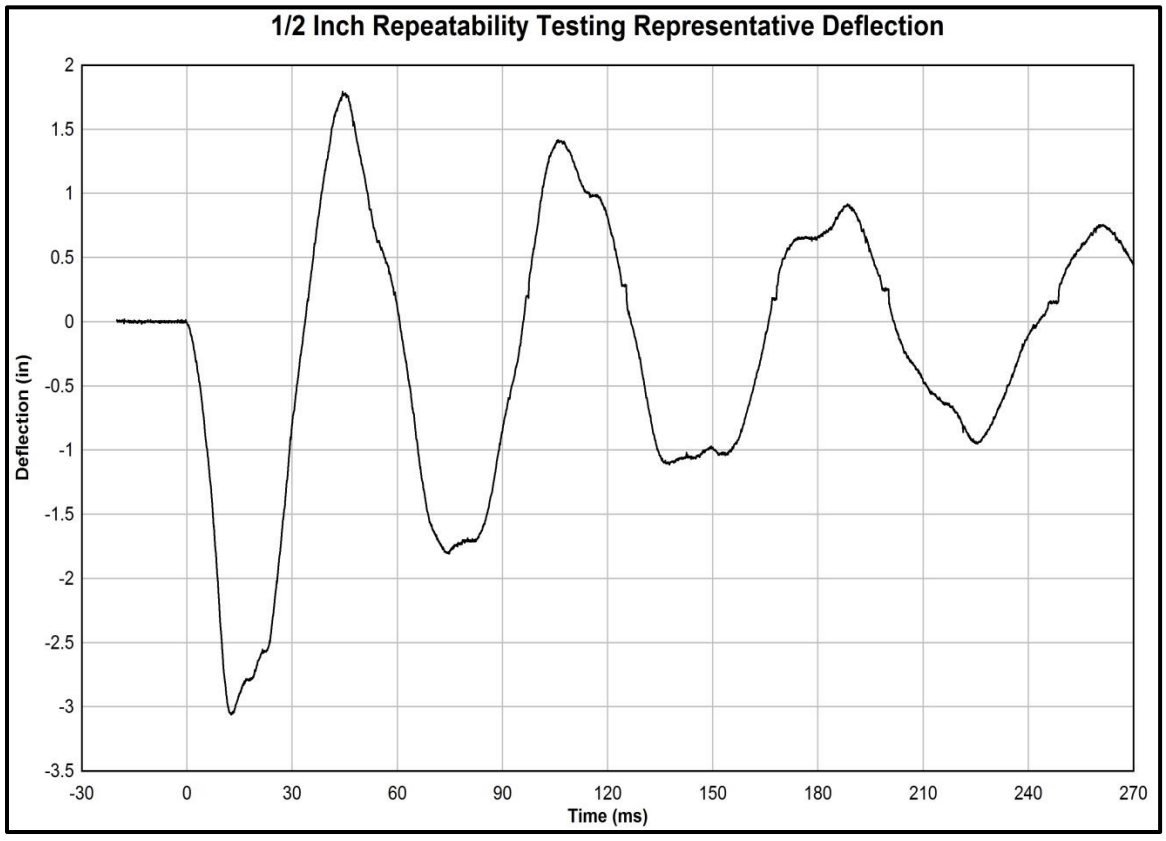

Figure 6.4: 1/2 Inch Polycarbonate Repeatability Testing representative deflection time curve

Table 6.4: 1/2 Inch Repeatability Testing Peak Deflection and Time

Blast Event		Peak Deflection	
System Type	Test #	Deflection (in)	Time (ms)
1/2" Poly	1	-3.038	12.6
1/2" Poly	2	-3.069	12.3
1/2" Poly	3	-3.062	12.6
1/2" Poly	4	-3.038	12.3
1/2" Poly	5	-3.066	12.6
	Average	-3.055	12.48
	Standard Deviation	0.015	0.16
	Maximum	-3.069	12.60
	Minimum	-3.038	12.30

6.3 Reaction Results

The Z-axis reaction forces recorded over the five 1/4 inch polycarbonate repeatability tests are summarized in Table 6.5 below. Positions D and E were located at the midpoint on the left side of the glazing system and positions Q and R were located on the right side as viewed from the outside of the shocktube. No data for position E was recorded due to the faulty load cell. Reaction forces seemed to be fairly consistent with the greatest standard deviation being equal to 55.12 lbf or 16.28% of the average load found at position Q. The shape of the reaction curves remained fairly consistent. A typical Z-axis loading curve can be found in Figure 6.5. This graph was taken from Position D, Test 2 and is representative of the reaction curves recorded during repeatability testing, however magnitudes did vary.

Table 6.5: 1/4 Inch Polycarbonate Repeatability Testing Z-Axis Loading

1/4 Inch Polycarbonate Repeatability Testing													
	Maximum Positive Z- Axis Loading												
Position	Test #	Force (lbf)	Test #	Force (lbf)	Test #	Force (lbf)	Test #	Force (lbf)	Test #	Force (lbf)	Avg Force (lbf)	Standard Deviation (lbf)	% Std Deviation
D	1	280.15	2	341.75	3	405.90	4	349.87	5	375.96	344.42	46.75	13.57
E		-		-		-		-		-	-	-	-
Q	1	301.40	2	343.12	3	365.26	4	344.40	5	450.40	338.55	55.13	16.28
R		299.12		340.18		307.92		274.40		301.63	305.40	23.60	7.73

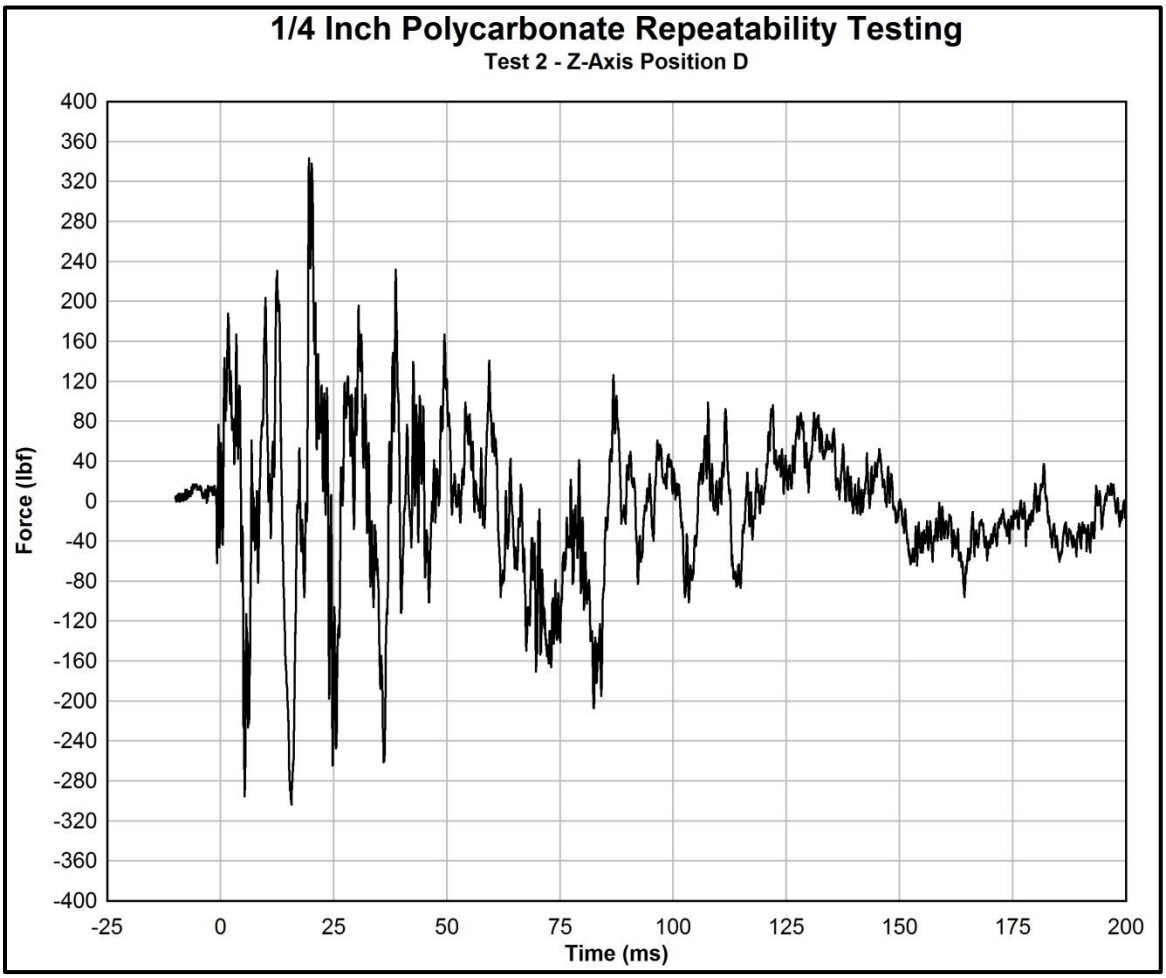

Figure 6.5: Representative 1/4 Inch Repeatability Testing Z-Axis Loading

The Z-axis reaction forces recorded over the five 1/2 inch polycarbonate repeatability tests are summarized in Table 6.6 below. Like the 1/4 inch tests, no data was recorded at position E. Data recorded at positions Q and R remained

fairly consistent. Position D experienced one significant anomaly during Test 4. A value of 421.821 lbf was recorded while the other tests recorded values ranging from 211.27lbf to 269.32 lbf. When comparing the reaction force curve of Test 4 to the other reaction forces curves at position D, no clear reason for the anomaly can be observed. The curve exhibits the same shape characteristics with the exception of a much higher magnitude. Figure 6.6 shows a reaction force curve typical of the results recorded during 1/2 Inch Polycarbonate Repeatability Testing.

Table 6.6: 1/2 Inch Polycarbonate Repeatability Testing Z-Axis Loading

1/2 Inch Polycarbonate Repeatability Testing													
	Maximum Positive Z- Axis Loading												
Position	Test #	Force (lbf)	Test #	Force (lbf)	Test #	Force (lbf)	Test #	Force (lbf)	Test #	Force (lbf)	Avg Force (lbf)	Standard Deviation (lbf)	% Std Deviation
D	1	250.354	2	269.323	3	211.272	4	421.821	5	217.724	288.19	85.93	29.82
E		-		-		-		-		-	-	-	-
Q	1	535.121	2	502.235	3	654.321	4	665.2	5	634.738	589.22	74.43	12.63
R		276.885		232.091		246.334		228.32		212.829	245.91	24.16	9.83

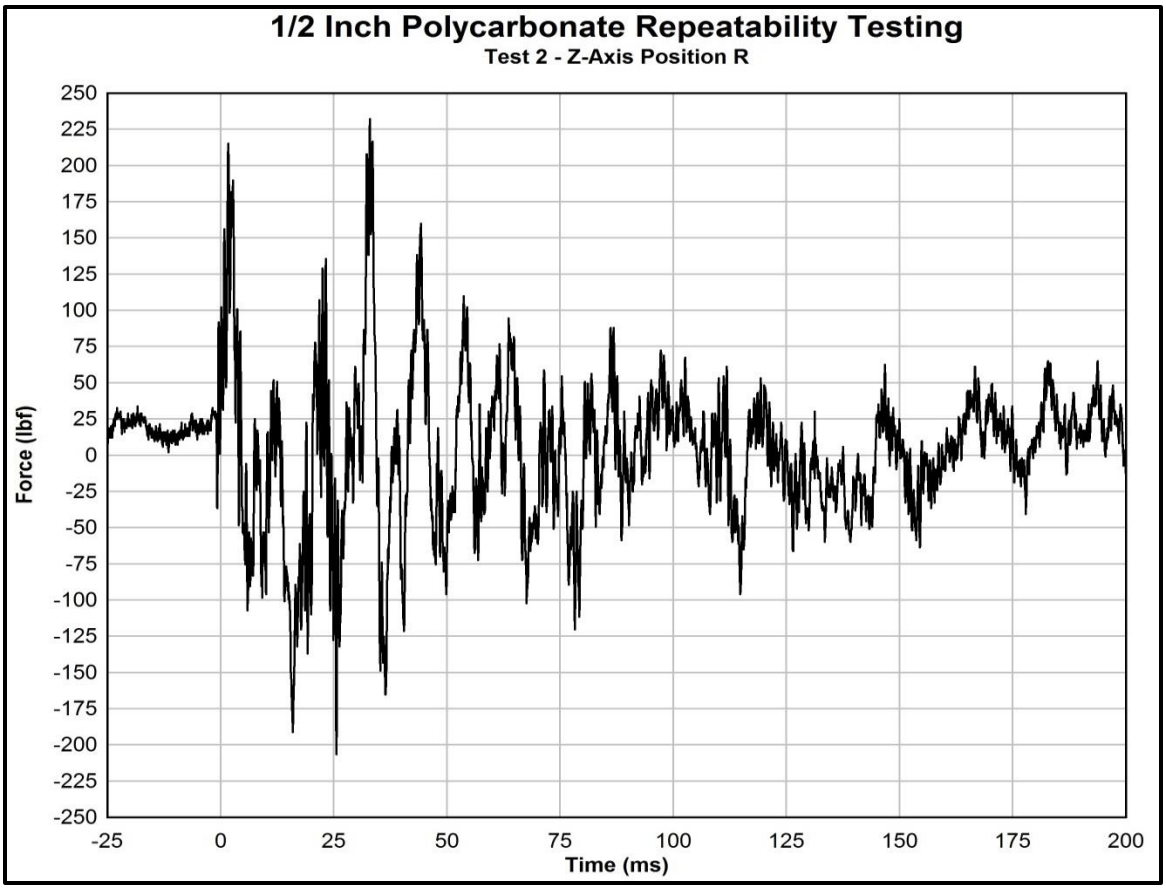

Figure 6.6: Representative 1/2 Inch Repeatability Testing Z-Axis Loading

Chapter Seven: Failure Testing Results and Analysis

Two tests were required to cause the 1/4 inch polycarbonate system to fail. Due to the extreme flexure of the system, the screws holding the frame to the attachment points sheared, allowing the system to fall back into the shock tube during the negative blast phase. The 1/2 inch polycarbonate system required three tests to cause failure. The mode of failure was similar to that of the 1/4 inch system. The flexure of the framing material caused a majority of the screws to shear resulting in the system being sucked 14 feet back into the shock tube, flipping in the process.

7.1 Pressure Results

7.1.1 Quarter Inch Polycarbonate

The first test, using a 400 gram charge at 77 feet, resulted in a maximum peak pressure of 6.437 psi and impulse of 47.809 psi-ms. This caused screws in nine of the 26 positions to shear, but the window remained in place. The second test, which resulted in the failure of the glazing system, achieved a peak pressure of 8.287 psi and impulse of 74.713 psi-ms. This was accomplished through the use of a 600 gram charge at 77 feet. It should be reiterated that glazing system itself did not fail, rather the screws holding the frame to the attachment points failed, allowing the glazing system to fall into the shock tube. A summary of the pressure results can be found in Table 7.1.

Table 7.1: 1/4 Inch Polycarbonate Failure Testing Peak Pressure and Impulse

Blast Event		Positive Phase Maximum Values					
System Type	Test #	Channel		Avg Peak Pressure	Channel		Avg Peak Impulse
		1	2		1	2	
1/4 Poly	1	6.553398	6.320437	6.437	47.92169	47.69621	47.809
1/4 Poly	2	8.287379	8.544643	8.416	73.92569	74.71277	74.319

In Figure 7.1, the 1/4 inch sample can be seen post failure. The glazing system remains largely intact with some deformation of the aluminum framing. Upon closer inspection, screw heads can still be found resting in the attachment points.

Figure 7.1: 1/4 inch polycarbonate post-failure

7.1.2 Half Inch Polycarbonate Failure Testing

Three tests were required to cause failure of the 1/2 inch polycarbonate system. As with the 1/4 inch system, it must be noted that the glazing system itself did not fail, rather the screws attaching the framing to the attachment points failed. Had they not failed, it is uncertain how much more loading the glazing system may have been able to withstand. The first test used a 400 gram charge at 77 feet. This resulted in a pressure of 6.799 psi and impulse of 49.591 psi-ms. There was no noticeable damage to the glazing system following this test. The following test used a 600 gram charge, again at 77 feet. This resulted in a pressure of 8.355 psi and impulse of 77.823 psi-ms. Damage to the glazing system was limited to some slight bending of the framing material concentrated near the attachment points. The final test, which achieved a peak pressure of 10.454 psi and impulse of 120.923 psi-ms, resulted in the glazing system failing and being sucked 14 feet back into the shock tube. A 900 gram charge at 77 feet was used for this test. The pressure and impulse results are summarized in the table below.

Table 7.2: 1/2 Inch Polycarbonate Failure Testing Peak Pressure and Impulse

Blast Event		Positive Phase Maximum Values					
System Type	Test #	Channel		Avg Peak Pressure	Channel		Avg Peak Impulse
		1	2		1	2	
1/2 Poly	1	6.875728	6.722222	6.799	49.37769	49.8037	49.591
1/2 Poly	2	8.335922	8.374008	8.355	77.58019	78.06545	77.823
1/2 Poly	3	10.56505	10.34226	10.454	120.2463	121.6001	120.923

In Figure 7.2, the 1/2 inch polycarbonate sample can be seen post-failure. Again, the glazing system remains largely intact with only slight deformation of the aluminum framing. The greatest damage was caused by screw pullout.

Figure 7.2: 1/2 inch polycarbonate sample post-failure

7.2 Reaction Results

7.2.1 Quarter Inch Polycarbonate

A summary of the Z-axis reaction forces can be found in Table 7.3 along with the pressure and impulse associated with each of the two tests. The reaction forces increased from Test 1 to 2 as anticipated with the exception of position D, in which case the peak loading decreased from 1058.17 lbf in test 1 to 770.32 lbf in test 2. The reason for this is unknown as the reaction force curve does not exhibit any abnormalities. It is possible that a greater percentage of the loading was transferred to an adjacent attachment point but without instrumentation this cannot be verified. A typical reaction force curve associated with the 1/4 Inch Polycarbonate Failure Testing is shown in Figure 7.3.

Table 7.3: Reaction force loading for 1/4 Inch Polycarbonate Failure Testing

1/4 Inch Polycarbonate Failure Testing				
Maximum Positive Z- Axis Loading				
Position	Test #1 Pressure/ Impulse	Test #1 Force (lbf)	Test #2 Pressure/ Impulse	Test #2 Force (lbf)
D	6.437 psi / 47.696 psi-ms	1058.17	8.416 psi / 74.319 psi-ms	770.32
E		-		-
Q		646.23		929.76
R		440.30		765.82

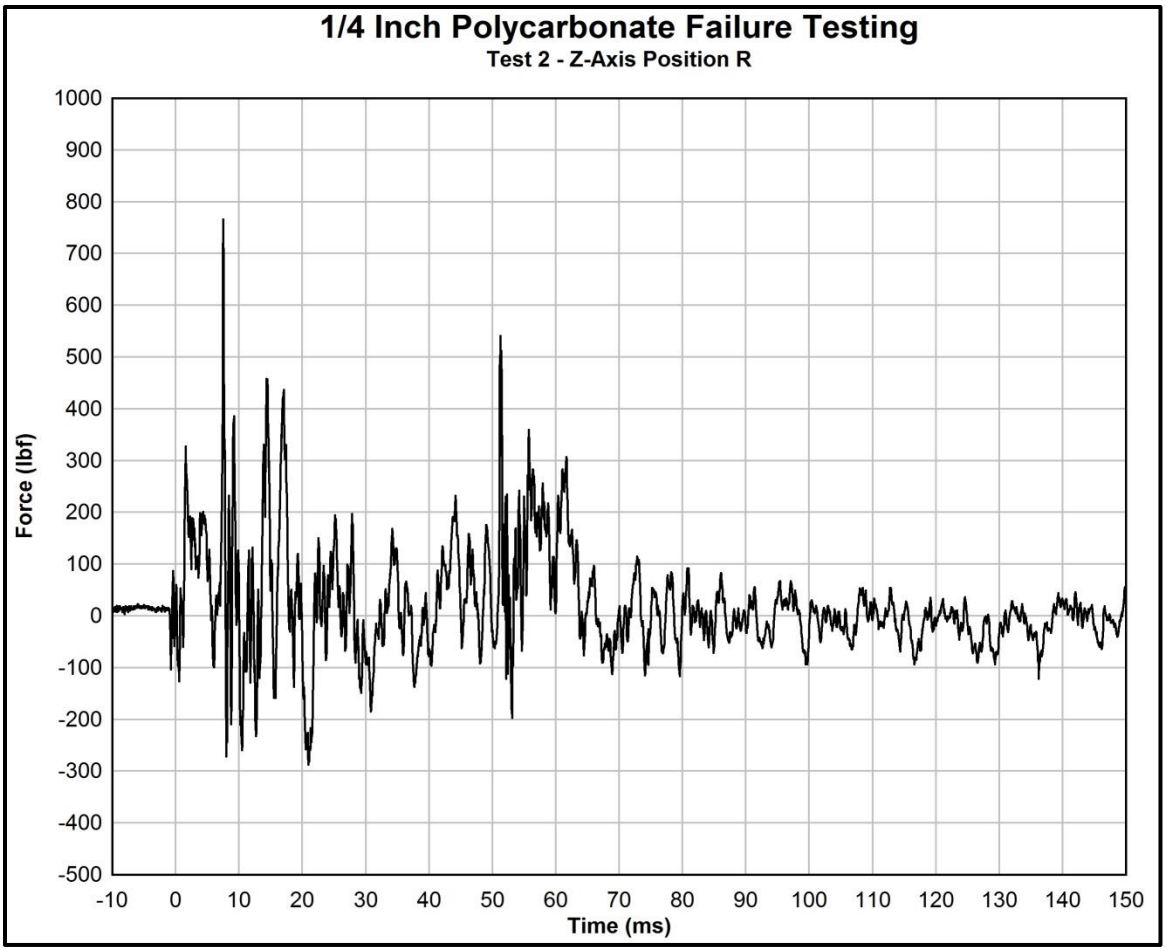

Figure 7.3: Representative reaction force curve from 1/4 Inch Polycarbonate Failure Testing

7.2.2 Half Inch Polycarbonate

A summary of the Z-axis reaction forces can be found in Table 7.4 along with the pressure and impulse associated with each of the three tests. The reaction force results are as expected with the loading increase for each test until the sample failed. There was a slight deviation in the data for Test 2, position D, with the peak value decreasing slightly from Test 1 to Test 2. However, the value did increase for Test 3. As with 1/4 inch failure testing, the reason for this decrease cannot be explained. A typical reaction force curve for 1/2 Inch Polycarbonate Failure Testing is shown in Figure 7.4.

Table 7.4: Reaction force loading for 1/2 Inch Polycarbonate Failure Testing

1/2 Inch Polycarbonate Failure Testing						
Maximum Positive Z- Axis Loading						
Position	Test #1 Pressure/ Impulse	Test #1 Force (lbf)	Test #2 Pressure/ Impulse	Test #2 Force (lbf)	Test #3 Pressure/ Impulse	Test #3 Force (lbf)
D	6.799 psi / 49.591 psi-ms	483.32	8.355 psi / 77.823 psi-ms	474.34	10.454 psi / 120.923 psi-ms	827.63
E		-		-		-
Q		718.18		742.87		1186.01
R		372.43		430.25		642.40

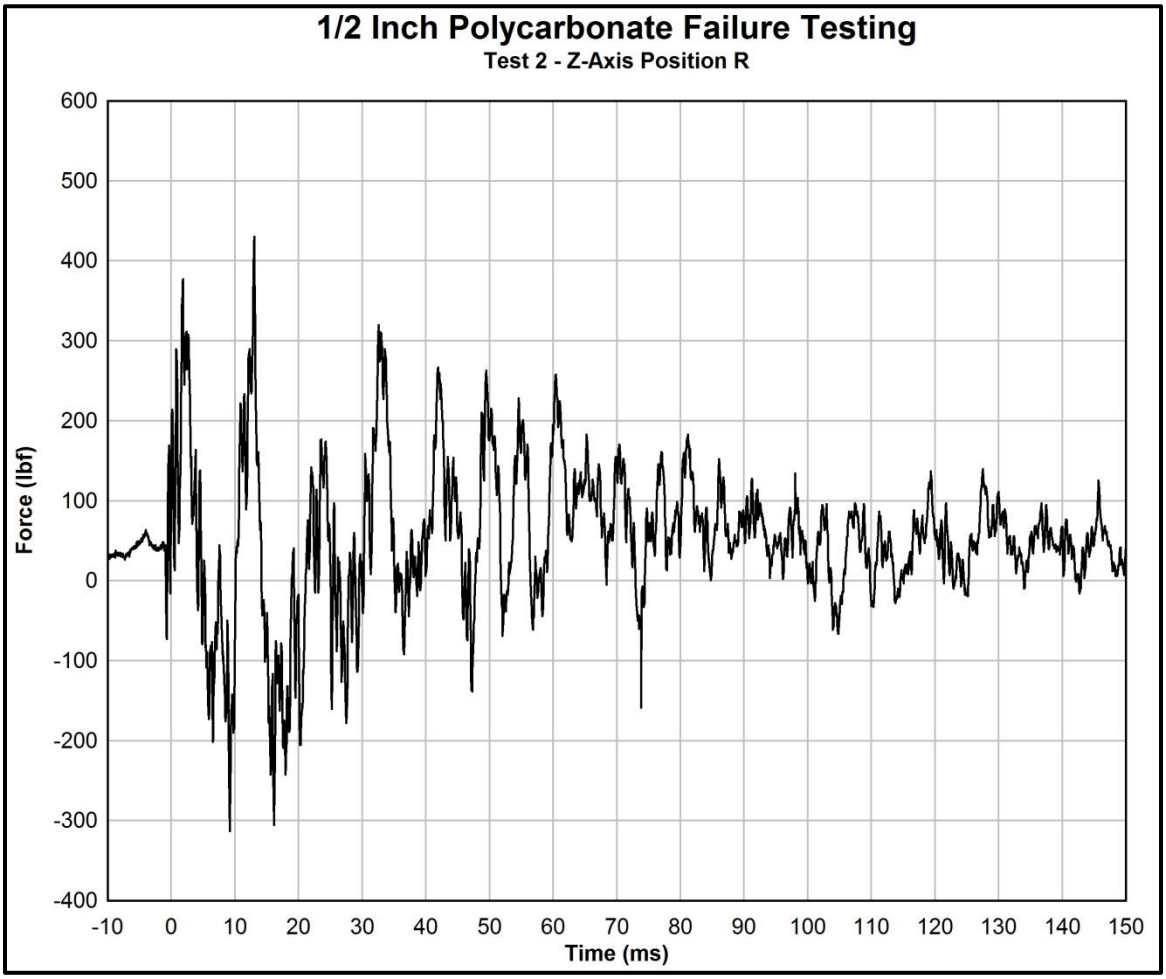

Figure 7.4: Representative reaction force curve from 1/2 Inch Polycarbonate Failure Testing

Chapter Eight: Comparizon to HazL Modeling

Window Fragment Hazard Level Analysis, or HazL, is a software program developed by the United States Army Corps of Engineers Protective Design Center. This program performs a single degree of freedom (SDOF) analysis on a blast resistant glazing system to calculate the glazing response to blast loading. It also employs a debris transport model for predicting fragment trajectory. HazL has the capabilities of modeling a variety of different glazing types including monolithic glass, laminated glass, polycarbonate, and windows retrofitted with anti-shatter film. Input parameters such as blast load, window geometry, and glazing type and thickness can be entered. HazL is then able to output the hazard level, glazing response, and reaction loads. The HazL user interface is shown in Figure 8.1.

Figure 8.1: HazL User Interface

8.1 Quarter Inch Polycarbonate Analysis

The first sample analyzed using the HazL program was the 1/4 inch polycarbonate blast resistant glazing system. Using a representative blast waveform from the experimental test series as the input blast loading yielded interesting results. With a peak pressure of 4.7 psi and impulse of 21.0 psi-ms, HazL predicts failure of the sample with the glazing pulling out of the frame. As was shown through multiple experimental tests, the 1/4 inch sample survived this loading with very minimal damage. In fact, a loading of 8.416 psi/74.319 psi-ms was required to cause pullout of the screws holding the glazing system to the attachment points, in which case the glazing still remained in the frame. Table 8.1 summarizes the HazL predicted reaction forces versus the reaction forces determined experimentally. As shown in the table, HazL greatly overpredicted the reaction forces. Another interesting result presented by HazL was peak deflection of the glazing. Through experimental results it was shown that the average peak deflection was 4.113 inches. HazL predicted a peak deflection of 5.185 inches at the time of failure.

Table 8.1: Comparison of HazL output to experimental results

1/4 Inch Comparison				
	HazL Results		Experimental Results	
	Reaction Force (lbf)	Peak Loading (lbs/in)	Reaction Force (lbf)	Peak Loading (lbs/in)
Long Edge	959.64	14.54	640.27	9.70
Short Edge	627.44	13.14	338.18	7.08

A number of different theoretical blast loading scenarios were run using HazL until a loading was found that did not cause failure. This loading had a pressure of 0.70 psi and 5.25 psi-ms with a positive phase duration of 15 ms, in which case HazL still predicted a peak deflection of 3.58 inches at 22.17 ms. Obviously, HazL overpredicts the deflection of the 1/4 inch polycarbonate, leading it to predict failure of the glazing system prematurely.

8.2 Half Inch Polycarbonate Analysis

The 1/2 inch polycarbonate glazing system was also analyzed using HazL in the same manner. Using the same typical blast waveform, HazL predicted that the sample would survive; however, the peak deflection was overstated at 3.939 inches compared to 3.002 inches witnessed experimentally. A summary of the HazL predicted reaction forces versus experimental reactions forces is shown in Table 8.2. In this case, HazL predicted reaction forces roughly two times higher than those predicted for the 1/4 inch sample. However, experimental results showed that the Z-axis reaction forces decreased from the 1/4 inch sample to the 1/2 inch sample.

Table 8.2: Comparison of HazL output to experimental results

1/2 Inch Comparison				
	HazL Results		Experimental Results	
	Reaction Force (lbf)	Peak Loading (lbs/in)	Reaction Force (lbf)	Peak Loading (lbs/in)
Long Edge	2269.08	34.38	537.66	8.15
Short Edge	1298.32	27.19	289.55	6.07

Following this analysis, different theoretical blast loading scenarios were run to determine when HazL would predict failure of the glazing system. This occurred using a loading of 8.00 psi and 120.00 psi-ms, similar to the 10.454 psi/120.923 psi-ms loading which caused failure experimentally. HazL predicted 5.185 inches of deflection and the glazing pulling out of the frame at failure. Although the blasting loadings were similar, the author believes that HazL prematurely predicts failure due to the fact that the experimental failure was the result of screw pullout, not glazing pullout.

Chapter Nine: Comparison to Laminated Glass Study

The results collected during the polycarbonate study are compared to the results and conclusions gathered during the laminated glass study conducted as part of the thesis completed by W.C. Wedding (Wedding, 2010). The laminated glass sample studied was equal in size to the polycarbonate samples studied and also used the same framing construction. The laminated glass was composed of two 1/8" panes of heat strengthened glass bonded together with a 0.060" thick layer of Uvekol. Figure 9.1 shows the laminated glass blast resistant glazing system installed in the test buck.

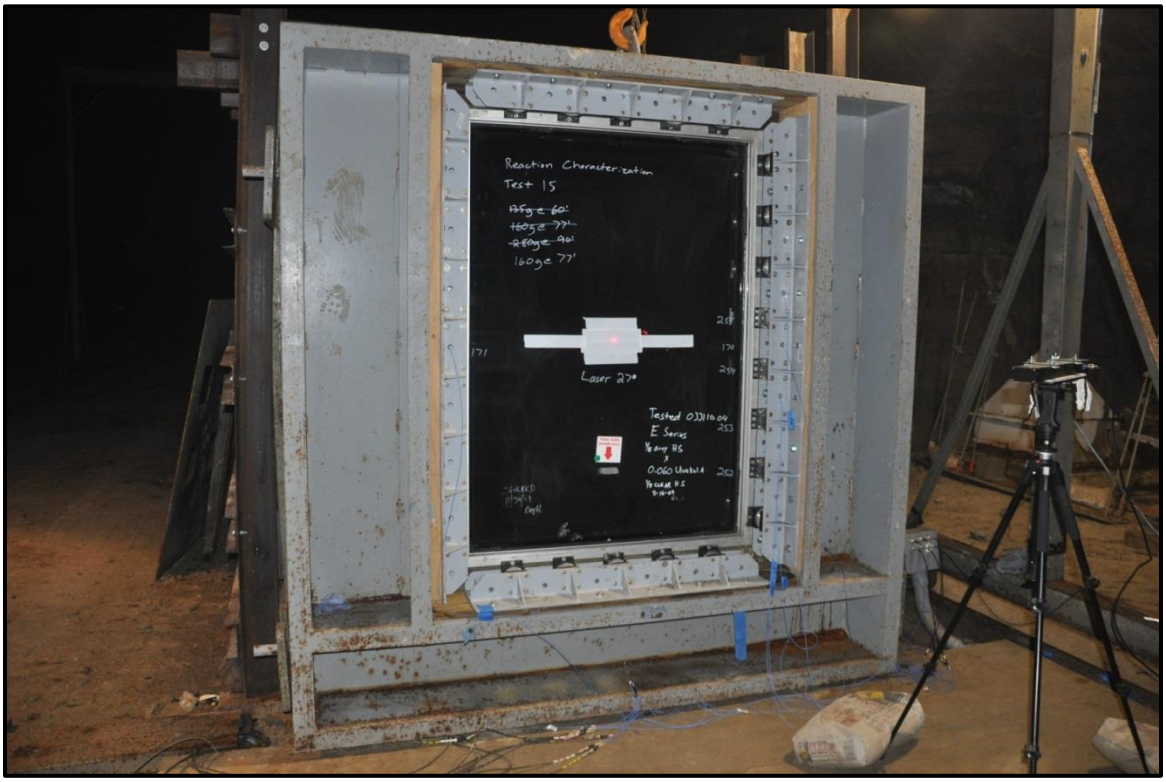

Figure 9.1: Laminated glass blast-resistant glazing system installed in buck (W.C. Wedding, 2010)

9.1 Deflection Comparison

Looking at the deflection versus time curve of each of the three glazing samples gives a better understanding of how the samples responded to blast loading. Figure 9.2 shows the three deflection time curves together. From this it can be seen that the laminated glass peaks quickest and has the lowest magnitude. This is followed by the 1/4 inch polycarbonate which has the greatest deflection and finally the 1/2 inch polycarbonate. The peak deflection towards the blast also follows the same pattern with laminated glass peaking first, followed by 1/4 inch and 1/2 inch polycarbonate. A summary of the peak deflections and respective times can be found in Table 9.1.

Table 9.1: Comparison of peak deflections and time of peak deflection

Deflection Comparison		
	Peak Deflection (in)	Time (ms)
1/4 Inch Laminated Glass	-1.22	9.27
1/4 Inch Polycarbonate	-4.12	10.03
1/2 Inch Polycarbonate	-3.00	12.34
HazL Predicted - 1/4" Poly	-3.96	6.97
HazL Predicted - 1/2" Poly	-3.94	15.59

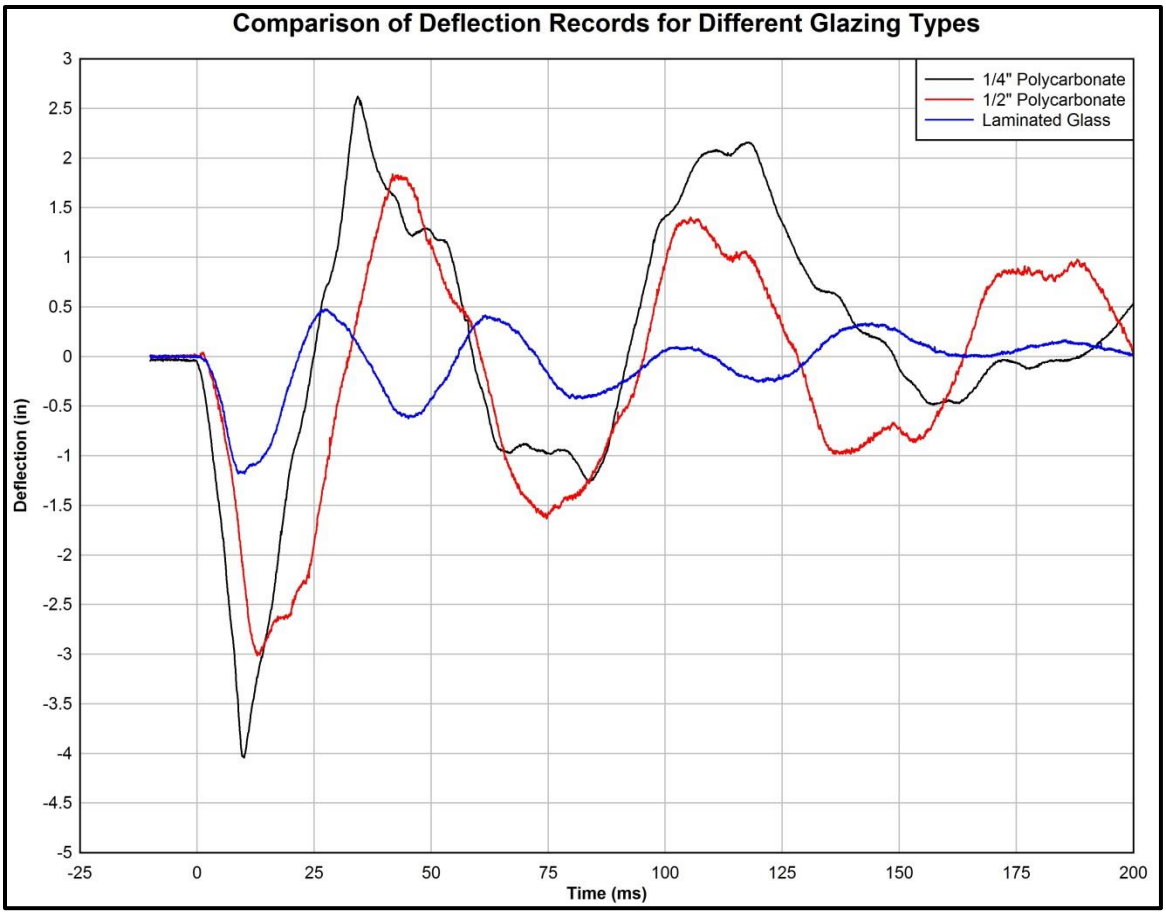

Figure 9.2: Comparison of deflection curves for polycarbonate and laminated glass samples

9.2 Reaction Comparison

A summary of the peak positive Z-axis reaction forces can be found in Table 9.2. This data is also shown graphically in Figure 9.3 with positions omitted where polycarbonate data was not available. Investigation of the data does not yield any discernible patterns. A major difference is noticed at positions H and N, the upper most points on the left and right sides, where the reaction forces are considerably higher for the polycarbonate samples than the laminated glass sample. At position H, the average polycarbonate value is 1069.39 lbf

while the laminated glass value is 163.10 lbf, equivalent to 15.25% of the polycarbonate value. Position N follows this trend with an average polycarbonate loading of 1016.29 lbf and a laminated glass value of 219.37 lbf or 21.59% of the polycarbonate value.

Table 9.2: Comparison of peak Z-axis reaction forces

Position	Glazing Type		
	1/4 Inch Polycarbonate Avg Force (lbf)	1/2 Inch Polycarbonate Avg Force (lbf)	1/4 Inch Laminated Glass Avg Force (lbf)
A			340.57
B			296.70
C			325.20
D	314.37	360.14	425.07
E	439.05	287.35	351.90
F			388.27
G			332.07
H	1173.69	965.09	163.10
I	601.53	461.33	357.75
J			297.70
K	230.57	271.60	265.47
L			252.87
M			360.30
N	1138.77	893.80	219.37
O			318.93
P			267.70
Q	401.59	458.28	327.07
R	374.11	261.33	350.90
S			287.83
T			309.37
U			218.10
V	371.83	265.11	250.17
W			276.17
X	233.15	243.07	347.20
Y			329.70
Z	175.95	129.71	215.17

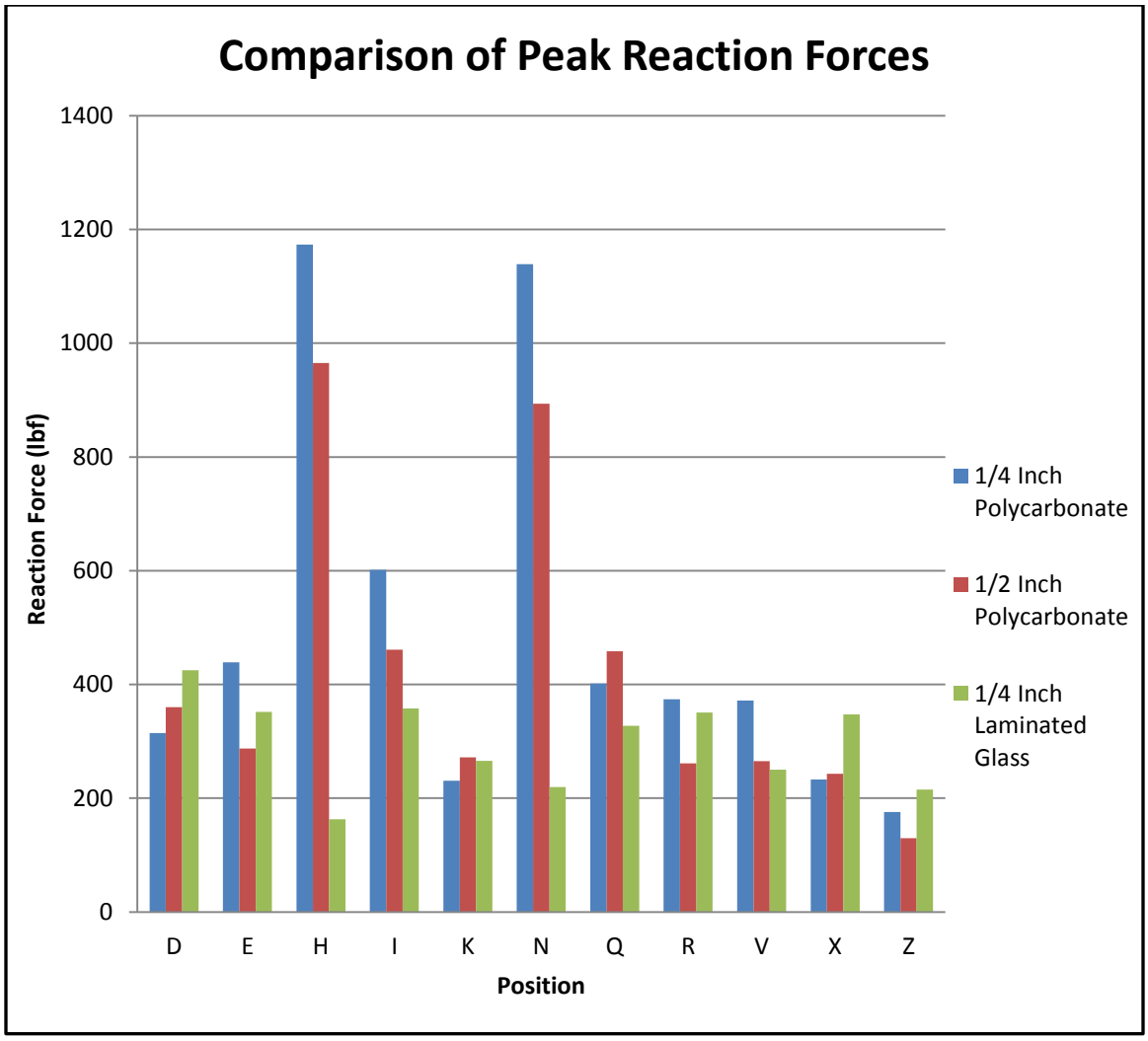

Figure 9.3: Comparison of peak positive Z-axis reaction forces

Based on the results presented by W.C. Wedding (Wedding, 2010), it was shown that laminated glass appeared to have higher Z-axis loadings concentrated at the midpoint of each long edge rather than at the corners. This study has shown that polycarbonate has higher Z-axis loads concentrated at the corners of the long edges. Also shown in the laminated glass study, is that laminated glass exhibits loads directly opposing one another on the short edges.

This can be seen in Figure 9.4. Polycarbonate did not seem to exhibit this same load distribution. Instead the loads were much more varied.

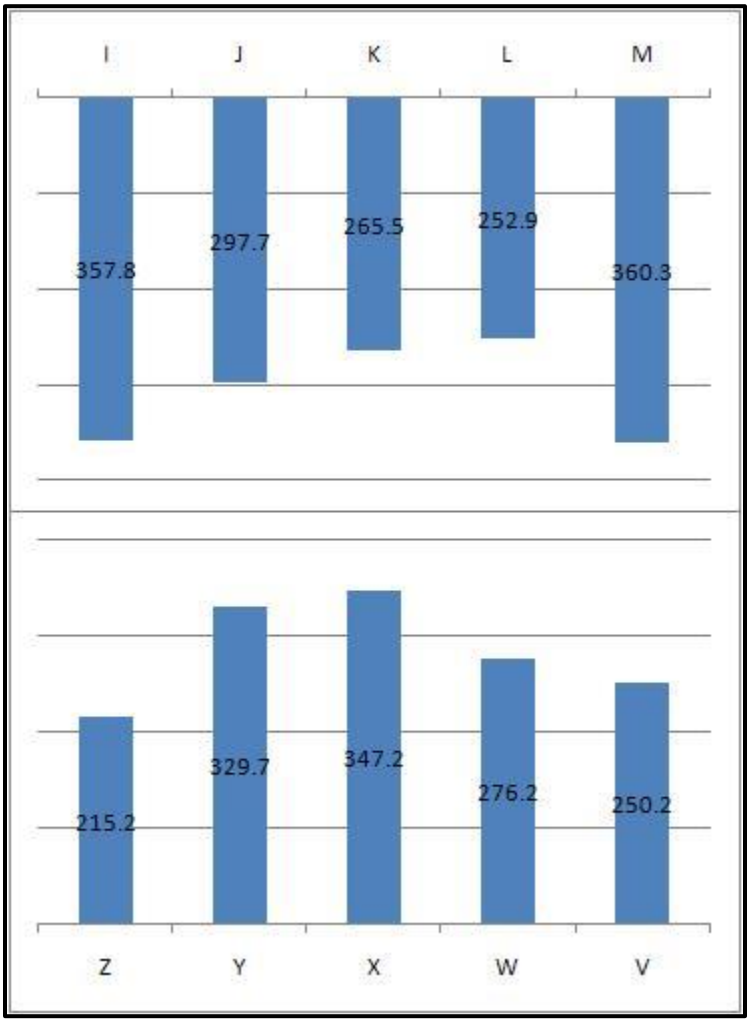

Figure 9.4: Laminated glass short edge load distribution (Wedding, 2010)

Chapter Ten: Conclusions

Perimeter testing results have shown that the reaction force distribution of polycarbonate differs significantly from that of laminated glass along the Z-axis. However, different thicknesses of polycarbonate do exhibit the same load distributions, albeit at different magnitudes. It was also shown that the X and Y axis reaction forces should be considered as they are generally of significant magnitude. Another point presented was that testing of a single polycarbonate sample should be limited as residual stresses are likely to accumulate, leading to permanent deformation and possibly erroneous data. Finally, it was shown that it may be possible to predict the load distribution around the perimeter of the glazing system by instrumenting only a limited number of points. However, future testing of additional polycarbonate panels of differing thickness and sizes would be required to validate this hypothesis.

HazL was used to analyze each of the polycarbonate glazing systems and provided results that did not correspond well with test data. In the case of the 1/4 inch polycarbonate, HazL dramatically underpredicted the failure point, predicting that the sample would fail at blast loadings of less than 1 psi, when in fact the sample survived 19 tests at pressures of 4.5 psi or greater. Hazl also overpredicted peak deflection and peak loading at failure. The analysis of 1/2 inch polycarbonate presented the same trends. If supporting members are designed using only the blast loadings at which HazL predicts polycarbonate glazing system failure, they may be dramatically undersized. This could result in

severe damage to the support members and transmit greater than anticipated loads down the load path, resulting in progressive collapse of the structure.

It was shown through these results that it is not possible to rely on HazL to provide accurate results for polycarbonate. It was also shown that it may be possible to predict the Z-axis load distribution around the perimeter of a polycarbonate sample using a limited number of tests; however, additional testing is required to verify this possibility. Based on these conclusions, the only currently acceptable solution to accurately validate the design of polycarbonate blast resistant glazing systems is to subject samples to blast loading to determine glazing resistance. The tests should be conducted in manner consistent with real world applications, and the samples should be tested to failure.

References

AAMA, 2006, “Voluntary Guide Specification for Blast Hazard Mitigation for Fenestration Systems,” AMMA 510-06, Schaumburg, IL.

ASTM, 2003, “Standard practice for specifying an equivalent 3-s duration design loading for blast resistant glazing fabricated with laminated glass,” *F 2248-03,* West Conshohocken, PA.

ASTM, 2004a, “Standard practice for determining the load resistance of glass in buildings,” *E 1300-04,* West Conshohocken, PA.

ASTM, 2004b, “Standard test method for glazing and glazing systems subjected to airblast loadings,” F 1642-04, West Conshohocken, PA.

ASTM, 2012a, “Standard practice for determining the load resistance of glass in buildings,” E 1300-12, West Conshohocken, PA.

ASTM, 2012b, “Standard practice for specifying an equivalent 3-s duration design loading for blast resistant glazing fabricated with laminated glass,” *F 2248-12,* West Conshohocken, PA.

CoE, Waterways Experiment Station, 1992. “Airblast Testing of Blast Resistant Window Systems,” Technical Report SL-92-8. Corps of Engineers, Vicksburg, MS.

DoD, 2003, “Department of Defense Minimum Antiterrorism Standoff Distances for Buildings,” Unified Facility Criteria (UFC) 4-010-01,US Department of Defense, Washington DC.

DoD, 2012, “Department of Defense Minimum Antiterrorism Standoff Distances for Buildings,” Unified Facility Criteria (UFC) 4-010-01 9 February 2012,US Department of Defense, Washington DC.

DoS, Bureau of Diplomatic Security, 1987. “Design of Structures to Resist Terrorist Attack, Report 2, Full-Scale Perimeter Wall and Window Test.” Department of State, Washington, DC.

DoS, Bureau of Diplomatic Security, 1989. “Design of Structures to Resist Terrorist Attack, Report 5, Embassy Window and Door Blast Standards Verification Program.” Department of State, Washington, DC.

Dusenburry, D.O, Ed., 2010, Handbook for Blast-Resistant Design of Buildings. John Wiley & Sons, Inc.

GSA, 2003, “Standard Test Method for Glazing and Window Systems Subject to Dynamic Overpressure Loadings,” GSA-TS01-2003.

HazL, 1998, https://pdc.usace.army.mil/software/hazl/, Protective Design Center, Omaha District Corps of Engineers, Omaha, NE.

Hooper, P. A., et al., 2011, "On the blast resistance of laminated glass." International Journal of Solids and Structures 49: 899-918.

Meyers, G.E., 1986. “User Data Package for Blast Resistant Windows,” TM 51-86-23. Naval Civil Engineering Laboratory, Port Hueneme, CA.

Meyers, G. E., et al. ,1994, State of the Art of Blast Resistant Windows. Twenty-Sixth DoD Explosives Safety Seminar, Miami, FL.

Ngo, T., Mendis P., Gupta A., and Ramsay, J., 2007, “Blast loading and blast effects on structures – an overview,” *Electronic Journal of Structural Engineering*, Special Issue, Vol. 7, pp. 79 – 91.

Norville, H. Scott, and Conrath, Edward J., 2001, “Considerations for blast-resistant glazing design,” *Journal of Architectural Engineering,* September, Vol. 7, No. 3. pp. 80 – 86.

Norville, H. Scott, and Conrath, Edward J., 2006, “Blast-resistant glazing design,” *Journal of Architectural Engineering,* September, Vol. 12, No. 3. pp. 129 – 136.

Stewart, M. G. and M. D. Netherton ,2008, "Security risks and probabilistic risk assessment of glazing subject to explosive blast loading." Reliability Engineering & System Safety 93(4): 627-638.

Stiles Custom Metal, Inc., 2010, Security Glass & Glazing Guide.

Wedding, W. C. ,2010, “Experimental Study of Blast Resistant Glazing System Response to Explosive Loading,”. Master’s Thesis, College of Engineering. University of Kentucky, Lexington, KY.

VITA

Joshua Thomas Calnan was born in Oneida, New York to Tom and Cori Calnan. As a child he moved to Statesville, North Carolina where he attended Mitchell Community College and received an Associate in Science. He then moved to Lexington, Kentucky to attend the University of Kentucky where he was awarded a Bachelor of Science in Civil Engineering degree. He then joined the Mining Engineering Department working as a graduate research assistant and teaching assistant under Dr. Braden Lusk. He expects to graduate with a Master of Science in Mining Engineering in May 2013. He has been a member of SME and ISEE since 2011.